1521-0103/383/1/32–43$35.00
THE JOURNAL OF PHARMACOLOGY AND EXPERIMENTAL THERAPEUTICS

dx.doi.org/10.1124/jpet.122.001301
J Pharmacol Exp Ther 383:32–43, October 2022

Cinnabarinic Acid Provides Hepatoprotection Against Nonalcoholic Fatty Liver Disease[S]

Nikhil Y. Patil, Iulia Rus, Emma Downing, Ashok Mandala, Jacob E. Friedman, and Aditya D. Joshi

Department of Pharmaceutical Sciences (N.Y.P., I.R., E.D., A.D.J.) and Harold Hamm Diabetes Center (A.M., J.E.F., A.D.J.), University of Oklahoma Health Sciences Center, Oklahoma City, Oklahoma

Received May 3, 2022; accepted July 12, 2022

ABSTRACT

Nonalcoholic fatty liver disease (NAFLD) is a chronic condition in which excess lipids accumulate in the liver and can lead to a range of progressive liver disorders including non-alcoholic steatohepatitis, liver cirrhosis, and hepatocellular carcinoma. While lifestyle and diet modifications have proven to be effective as NAFLD treatments, they are not sustainable in the long-term, and currently no pharmacological therapies are approved to treat NAFLD. Our previous studies demonstrated that cinnabarinic acid (CA), a novel endogenous Aryl hydrocarbon Receptor (AhR) agonist, activates the AhR target gene, Stanniocalcin 2, and confers cytoprotection against a plethora of ER/oxidative stressors. In this study, the hepatoprotective and anti-steatotic properties of CA were examined against free fatty-acid-induced in vitro and high-fat-diet fed in vivo NAFLD models. The results demonstrated that CA treatment significantly lowered weight gain and attenuated hepatic lipotoxicity both before and after the established fatty liver, thereby protecting against steatosis, inflammation, and liver injury. CA mitigated intracellular free fatty acid uptake concomitant with the downregulation of CD36/fatty acid translocase. Genes involved in fatty acid and triglyceride synthesis were also downregulated in response to CA treatment. Additionally, suppressing AhR and Stc2 expression using RNA interference in vitro verified that the hepatoprotective effects of CA were absolutely dependent on both AhR and its target, Stc2. Collectively, our results demonstrate that the endogenous AhR agonist, CA, confers hepatoprotection against NAFLD by regulating hepatic fatty acid uptake and lipogenesis.

SIGNIFICANCE STATEMENT

In this study using in vitro and in vivo models, we demonstrate that cinnabarinic acid (CA), an endogenous AhR agonist, provides protection against non-alcoholic fatty liver disease. CA bestows cytoprotection against steatosis and liver injury by controlling expression of several key genes associated with lipid metabolism pathways, limiting the hepatic lipid uptake, and controlling liver inflammation. Moreover, CA-induced hepatoprotection is absolutely dependent on AhR and Stc2 expression.

Introduction

Nonalcoholic fatty liver disease (NAFLD), distinguished by profuse acquisition of triglycerides in the liver, is the most prevalent chronic liver disease in the world (Le et al., 2021). NAFLD is often linked with obesity, type 2 diabetes, atherosclerosis, and cardiovascular diseases, increasing the risk of mortality (Angulo, 2002; Cohen et al., 2011; Wójcik-Cichy et al., 2018). The pathology of NAFLD can progress from hepatic steatosis to non-alcoholic steatohepatitis (NASH; steatosis with inflammation and fibrosis), to cirrhosis, hepatocellular carcinoma, and ultimately organ failure (Bugianesi et al., 2002; Farrell and Larter, 2006; de Alwis and Day, 2008; White et al., 2012; Cobbina and Akhlaghi, 2017). The mechanisms for the progression of NAFLD are complex and a multiple parallel hit hypothesis has been proposed to underlie the pathogenesis, which is not completely understood (Friedman et al., 2018). The onset of fatty liver disease is attributed to an imbalance in hepatic lipid homeostasis due to the elevated uptake of hepatic fat, increased de novo lipogenesis, reduced fat oxidation, and lipid export (Postic and Girard, 2008; Ipsen et al., 2018). Furthermore, excessive accumulation of lipids in hepatocytes can trigger oxidative stress, inflammation, apoptosis, and fibrosis, sequentially or simultaneously, leading to the progression of the disease (Day and James, 1998; Tilg and Moschen, 2010).

The ubiquitously expressed ligand-dependent transcription factor Aryl hydrocarbon Receptor (AhR) is known to play a role in xenobiotic metabolism and liver homeostasis (Mimura and Fujii-Kuriyama, 2003; Savouret et al., 2003; Park et al., 2005; Mitchell et al., 2006; Wu et al., 2007; Zhou et al., 2010). In the canonical pathway, ligand binding results in conformational changes and nuclear translocation of AhR, followed by

This work was supported by the National Institutes of Health National Institute of Diabetes and Digestive and Kidney Diseases [Grant R01-DK122028], and the Presbyterian Health Foundation – Harold Hamm Diabetes Center Seed Grant (to A.D.J.); and [Grant R01-DK121951] (to J.E.F.).
Authors report no conflict of interest.
dx.doi.org/10.1124/jpet.122.001301.
[S] This article has supplemental material available at jpet.aspetjournals.org.

ABBREVIATIONS: AhR, aryl hydrocarbon receptor; ALT, alanine aminotransferase; BSA, bovine serum albumin; CA, cinnabarinic acid; CD, control diet; HFD, high-fat diet; NAFLD, nonalcoholic fatty liver disease; NASH, nonalcoholic steatohepatitis; OA, oleic acid; PA, palmitic acid; Stc2, stanniocalcin 2; TCDD, dioxin, 2,3,7,8-tetrachlorodibenzo-p-dioxin.

the dimerization of AhR with the AhR nuclear translocator and binding to the xenobiotic response elements (GCGTG motif) present in the promoter region of AhR regulated genes (Reyes et al., 1992; Probst et al., 1993; Denison and Nagy, 2003; Wright et al., 2017). 2,3,7,8-tetrachlorodibenzo-p-dioxin (TCDD) is a prototypical exogenous AhR agonist of anthropic origin that is known to activate a plethora of detoxification genes, including cytochrome P450 1A1 (encoded by Cyp1a1) (Nebert et al., 1993; Ma, 2001; Ma et al., 2009). Recent studies examining the role of AhR in fatty acid metabolism and NAFLD reported that TCDD-induced AhR activation resulted in hepatic steatosis and fibrosis (Lee et al., 2010; Nault et al., 2016; Zhu et al., 2020). On the other hand, treatment with endogenous AhR agonists, indole and indole-3 acetic acid, attenuated steatosis (Hendrikx and Schnabl, 2019; Ji et al., 2019). We recently identified a tryptophan metabolite cinnabarinic acid (CA) as an endogenous activator of AhR that failed to induce hepatic Cyp1a1 but upregulated a novel AhR target gene, stanniocalcin 2 (Stc2), in the liver. Stc2 is a glycosylated peptide hormone involved in development, calcium regulation, angiogenesis, cell apoptosis, and proliferation (Joshi, 2020). CA treatment conferred protection against ethanol-induced liver steatosis, injury, and hepatocyte apoptosis in both acute and chronic models of alcoholic liver injury. However, its role in fatty acid or dietary high-fat-diet – induced lipotoxicity has not been studied previously.

In the current study we investigated the ability of the novel AhR ligand CA to protect specifically against palmitic and oleic-acid-induced in vitro and high-fat-diet (HFD)–fed in vivo NAFLD models, and identified potential molecular and metabolic pathways conferring the protection. Our data strongly suggest that CA treatment significantly reduced fatty acid deposition in oleic and palmitic acid treated HepG2 and AML12 cells. In a high-fat-diet–fed NAFLD model, CA administration reduced weight gain, alleviated hepatic steatosis, metabolic deterioration, liver triglyceride and cholesterol content, and mitigated liver injury. Moreover, CA treatment limited hepatic lipid uptake and fatty acid synthesis by downregulating expression of genes involved in fatty acid uptake, de novo lipogenesis, and triglyceride synthesis. Finally, the present study provides compelling evidence that the anti-steatotic properties exerted by CA are uniquely dependent upon AhR-activated Stc2 signaling.

Materials And Methods

Cell Culture and In Vitro Treatments. HepG2 (ATCC, HB-8065), the human hepatocellular carcinoma cell line, was grown in MEM medium (ThermoFisher Scientific, Waltham, MA) containing 10% fetal bovine serum (FBS) (R&D Biosystems, Minneapolis, MN) and 1% 100x penicillin-streptomycin solution (ThermoFisher Scientific), whereas differentiated non-transformed mouse hepatic cells, AML12 (ATCC, CRL-2254), were cultured in DMEM:F12 medium (ThermoFisher Scientific) supplemented with 10% FBS, 1% 100x ITS (ThermoFisher Scientific) containing insulin, transferrin, and selenium, 40 ng/ml dexamethasone (Millipore Sigma, St. Louis, MO), and 1% 100x penicillin-streptomycin solution. Cells were maintained in a humidified 5% CO_2 incubator at 37°C. Cells were treated with 500-μM BSA (Cayman Chemical, Ann Arbor, MI) + DMSO (control); 30-μM CA (CA-only) for 24 hours; 500-μM BSA-palmitate saturated fatty acid complex (palmitic acid, PA) or 500-μM BSA-oleate monounsaturated fatty acid complex (oleic acid, OA) for 24 hours (PA or OA-only); 30-μM CA and 500-μM PA or OA simultaneously for 24 hours (CA+PA or CA+OA); and 500-μM PA or OA for 24 hours followed by 30-μM CA treatment for an additional 24 hours (CA after PA or CA after OA). For in vitro knockdown studies, HepG2 cells were transfected with 50-nM Dharmacon SMARTpool ON-TARGETplus AhR siRNA, Stc2 siRNA, and non-targeting siRNAs (NT siRNA) (Horizon Discovery, Boyertown, PA) for 24 hours using DharmaFECT 4 transfection reagent according to the manufacturer's instructions. Cells were further treated with control, CA-only, PA or OA-only, CA+PA or CA+OA, and CA after PA or CA after OA.

Animals and In Vivo Treatments. Eight-week-old female C57BL/6J mice (wild type, WT) (Jackson Laboratory, Bar Harbor, ME) were used in abidance with the guidelines of the Institutional Animal Care and Use Committee at the University of Oklahoma Health Sciences Center. Mice were housed in plastic cages with corn cob bedding in a climate- and temperature-controlled facility. One week after adaptation, mice were fed a normal control diet (CD) (D12450J) or a high-fat diet (HFD) (D12492) (Research Diet, New Brunswick, NJ) and randomly assigned to four groups (7 mice in each group): 1) CD, mice fed with control diet (10 kcal% fat) for 16 weeks; 2) HFD, mice on a high-fat diet (60 kcal% fat) for 16 weeks; 3) CA+HFD, mice fed with high-fat diet and treated with CA for 16 weeks; and 4) CA after HFD, mice fed with high-fat diet for 16 weeks with CA treatment initiated after 10 weeks of exposure to HFD for remaining six weeks. The Organic Chemistry Core (University of Texas Medical Branch, Galveston) synthesized and provided CA for the experiments. Mice received 12 mg/kg (body weight) CA three times a week on Monday, Wednesday, and Fridays via intraperitoneal (i.p.) injection. Both food and water were provided ad libitum. Mice weight and food intake were measured weekly for 16 weeks, after which the mice were euthanized via overdose of isoflurane followed by removal of vital organs as a secondary confirmation method. Blood samples were collected, and livers were excised and weighed.

Cell Viability Assay. To measure the effect of free fatty acids on cell viability, 2×10^4 cells were plated in a 96- well culture plate and treated with different concentrations (0, 100, 250, 500, 750, and 1000 μM) of OA or PA for 24 hours. Cell viability was measured using the RealTime-Glo MT Cell Viability Assay (Promega, Madison, WI) following the manufacturer's protocol.

Oil Red O Staining. Cells were seeded on Laboratory-Tek II chamber slides at 80% confluency as described earlier (Guo et al., 2020). Cells were washed with PBS, incubated in propylene glycol for 5 minutes, and incubated overnight in oil red O solution (abcam, Waltham, MA). Stained slides were further treated with 85% propylene glycol for 1 minute and rinsed twice with distilled water. The slides were then incubated in hematoxylin solution for 1–2 minutes to counterstain the nuclei, then rinsed thoroughly with tap water and two changes of distilled water. Cells were imaged with a Nikon ECLIPSE Ni epifluorescence microscope (Nikon, Melville, NY). Quantitation of lipid droplets was performed using ImageJ. Additionally, a colorimetric assay was performed to quantify the oil red O accumulation. Cells grown and treated in a 6-well plate were washed with PBS, and 400-μl isopropanol was added to each well to dissolve the oil red O. From each well, 100-μl aliquots were transferred to a 96-well plate and absorbance was measured at 500 nm on a Synergy 2 plate reader (Agilent, Santa Clara, CA).

Histologic Examination. To observe the pathologic changes, liver tissues were kept in 10% neutral buffered formalin and submitted to the Stephenson Cancer Center Tissue Pathology Core (University of Oklahoma Health Sciences Center) for paraffin embedding, sectioning, and H&E staining.

Measurement of Lipid Content. Triglycerides from cultured cell lysates, and liver tissue homogenates were measured using the Triglyceride-Glo Assay (Promega, Madison, WI). Cholesterol from the liver tissue samples was detected using the Cholesterol/Cholesterol Ester-Glo Assay (Promega). Intracellular fatty acid quantification in HepG2 and AML12 cells was performed using a fluorometric free fatty acid assay kit (abcam). To determine fatty acid uptake, a QBT fatty acid uptake kit (Molecular Devices, San Jose, CA) was used. All the

assays were performed as per manufacturer's instructions and fluorescence/luminescence measured using a Synergy 2 microplate reader (Agilent).

Glucose Tolerance Test. Mice were fasted for 6 hours before receiving an oral bolus of 2 gm of glucose (Sigma-Aldrich) per kilogram of body weight. Blood glucose measurements were performed using an Accu-check Guide Me meter (Roche, Indianapolis, IN) on blood samples taken from the tail vein at 0, 15, 30, 60, 90, and 120 minutes.

Alanine Aminotransferase Assay. The ALT activity kit (abcam) was used according to the manufacturer's protocol to fluorometrically measure the serum alanine aminotransferase (ALT).

RNA Isolation and Quantitative Real Time – Polymerase Chain Reaction (qRT-PCR). Total RNA was extracted from liver tissues or treated HepG2 and AML12 cells using TRIzol reagent (Thermofisher Scientific) and quantified. The iScript cDNA Synthesis Kit (Bio-Rad, Hercules, CA) was used to synthesize first-strand cDNA from 1 μg total RNA. Quantitative RT-PCR was performed using gene-specific primers (IDT, Coralville, IA) (Supplemental Table 1) and PowerUp SYBR Green Master Mix (ThermoFisher Scientific) on a StepOnePlus real time PCR system (ThermoFisher Scientific). The relative expression level of each sample was expressed as a fold change using 18S ribosomal RNA as a reference gene.

Western Blot Analysis. Whole tissue lysates were fractioned by SDS-PAGE electrophoresis (Bio-Rad) and transferred to low fluorescence PVDF membranes using a Trans-Blot Turbo system (Bio-Rad). Membranes were probed using AhR (Enzo Lifesciences, Farmingdale, NY) and Stc2 (ProSci Inc, Poway, CA) (Joshi et al., 2022) antibodies. Proteins were detected using fluorescently labeled secondary antibodies (Bio-Rad) followed by imaging using the ChemiDoc MP imaging system (Bio-Rad).

Chromatin Immunoprecipitation. Liver tissue extracted from the mice were fixed with 1% formaldehyde and subjected to chromatin-immunoprecipitation (ChIP) using the ChIP-IT Express Enzymatic Kit (Active Motif) as described previously (2022). The protein-bound DNA complexes were immunoprecipitated using antibodies against AhR (abcam, Cambridge, MA), IgG (negative control) (abcam), and histone H3 (positive control) (Cell Signaling Technology, Danvers, MA). Primers specific to the Cyp1a1 and Stc2 promoters (Supplemental Table 2) were used to PCR amplify the input and immunoprecipitated DNA. PCR products electrophoresed on 5% polyacrylamide gel and stained with SYBR green (ThermoFisher Scientific) were imaged using the ChemiDoc MP imaging system (Bio-Rad).

Statistical Analysis. Both in vitro and in vivo experiments performed—including animal/sample size, data acquisition methods, and data analysis protocols—were preset for this hypothesis-testing study (Michel et al., 2020). Animal numbers required were determined based on our previous observations and by using the G*Power statistical suite ($\alpha = 0.05$ and $\beta = 0.80$) (Faul et al., 2009). CA and free fatty acid treatments were performed using appropriate blinding methods and controls. Data were analyzed by applying multivariate ANOVA models, unless noted in the figure legends, using Sigma Plot software (Systat Software, San Jose, CA). After the overall significant F test from the mixed-effects multivariate ANOVA model, post hoc multiple comparison tests were performed for the prespecified comparisons adjusted by the Tukey procedure. All results are expressed as mean ± standard deviation (SD). Differences between the groups were considered significant only if the P value was < 0.05.

Results

CA Attenuates Steatosis in PA/OA-Treated HepG2 and AML12 Cells. To determine an optimal concentration of free fatty acids that mimic in vitro models of NAFLD without inducing overt cytotoxicity, a cell viability assay was performed in HepG2 and AML12 cells with varying concentrations of PA and OA. We observed that both PA and OA significantly decreased cell viability in HepG2 cells at concentrations higher than 500 μM (Fig. 1A), whereas in AML12 cells, significant cytotoxicity was observed at 750 μM (Supplemental Fig. 1A). Consequently, all subsequent in vitro experiments in HepG2 and AML12 cells were performed using 500-μM PA and OA concentrations. Our previous study determined the activation of AhR – as reflected by maximal induction of the AhR target gene, Stc2 – with 30-μM CA treatment for 24 hours (Joshi et al., 2015). Here, we examined the capability of CA to protect against PA/OA- induced steatosis in both HepG2 and AML12 cells. Oil red O staining indicated significant accumulation of lipids in both cell lines with 500-μM free fatty acid treatment, thus validating the in vitro NAFLD model used in the study (Fig. 1, B and C). Simultaneous treatment of CA with PA/OA as well as CA administration 24 hours after PA/OA treatment showed a significant reduction in steatosis both in HepG2 (Fig. 1, B and C) and AML12 (Supplemental Fig. 1, B and C) cells, as compared with the PA/OA-only treatment. The colorimetric oil red O measurement assay was corroborated with the aforementioned findings and confirmed the CA-attenuated PA/OA-induced lipid accumulation in both HepG2 (Fig. 1D) and AML12 (Supplemental Fig. 1D) cells.

CA Decreases Intracellular Lipid Accumulation in PA/OA-Treated In Vitro Model of NAFLD. An increase in the uptake of free fatty acids by hepatocytes and de novo lipogenesis is known to stimulate excess accumulation of intracellular triglycerides that causes hepatic steatosis and lipotoxicity (Kawano and Cohen, 2013). Therefore, we first measured the accumulation of total intracellular triglyceride and free fatty acid content in the presence of PA/OA-only as well as with CA treatment. Simultaneous and post-treatment with CA significantly alleviated the triglyceride and free fatty acid content in HepG2 (Fig. 2, A and B) and AML12 (Supplemental Fig. 2, A and B) cells. Concurrent CA treatment, CA + PA and CA + OA, reduced triglyceride levels by 53–65% and 51–66%, whereas CA treatment after PA/OA decreased cellular triglycerides by 35–43% and 37–47% in HepG2 and AML12 cells, respectively. Similarly, free fatty acid content in HepG2 and AML12 cells was reduced with CA treatment (Fig. 2B and Supplemental Fig 2B). Overall, simultaneous CA and PA/OA treatment resulted in a greater reduction in triglyceride and free fatty acid content as compared with CA administration 24 hours after free fatty acid treatment. To understand the effect of CA treatment on the mobility of long-chain fatty acids, an intracellular uptake of fluorescently labeled fatty acid analog, BODIPY-dodecanoic acid, was measured. CA treatment attenuated the uptake of free fatty acids in both HepG2 (Fig. 2C) and AML12 (Supplemental Fig. 2C) cells.

Downregulation of Genes Involved in Free Fatty Acid Uptake, Lipid Metabolism, and Inflammation with CA Treatment. To investigate the mechanism by which CA bestows its anti-steatotic effects, changes in the gene expression profiles of several key genes involved in lipid metabolism pathways were measured. Quantitative RT-PCR indicated upregulation of the fatty acid translocase CD36 in PA/OA-only treated cells, which was significantly reduced upon CA treatment (Fig. 3A and Supplemental Fig. 3A). Expression of genes involved in fatty acid synthesis, including acetyl-CoA carboxylase 1 (ACC1), fatty acid synthase (FASN), stearoyl-CoA desaturase 1 (SCD1), sterol

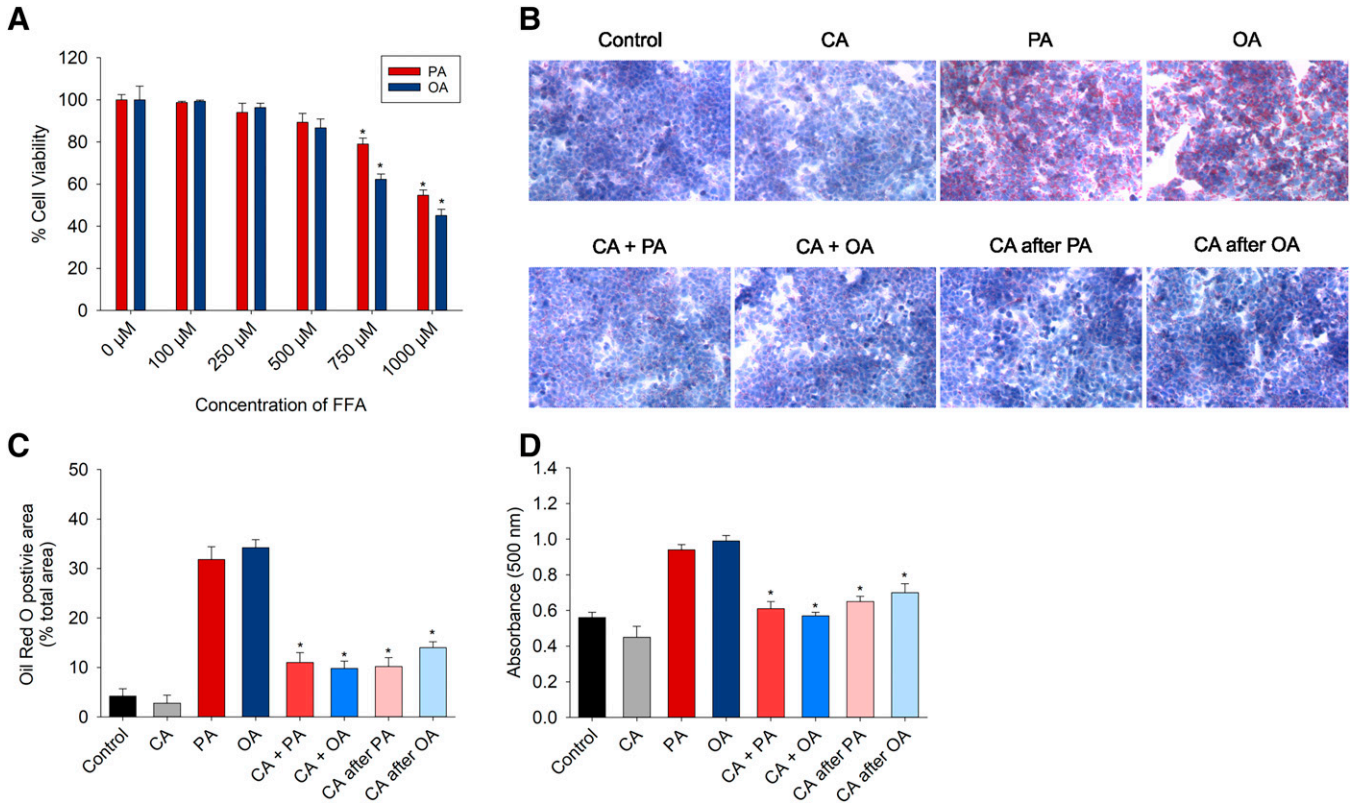

Fig. 1. Determination of (A) cell viability of HepG2 cells treated with different concentrations of palmitic acid (PA) and oleic acid (OA) for 24-hour cell viability was measured by a luminescent assay and expressed relative to BSA-treated control. Data are represented as mean ± SD ($n = 3$). *$P < 0.05$ compared with control group. (B) CA protects against palmitic acid (PA)/oleic acid (OA)-induced steatosis. Representative images of oil red O stained HepG2 cells treated with 500-μM BSA + DMSO (control), 30-μM CA, 500-μM PA, 500-μM OA, 30-μM CA+ 500-μM PA/OA, 30-μM CA after 500-μM PA/OA. (C) Quantification of oil red O-stained images; area of oil red O-stained lipid droplets was normalized to the total area (three images per treatment). (D) Quantification of accumulated oil red O by colorimetry; absorbance measured at 500 nm. Data are represented as mean ± SD ($n = 3$). *$P < 0.05$ compared with PA/OA-only treatment group.

regulatory element binding protein-1 (SREBP1), peroxisome proliferator-activated receptor gamma (PPARγ), and perilipin 2 (PLIN2), were increased with PA/OA treatments (Fig. 3B and Supplemental Fig. 3B). CA treatment attenuated expression of the aforementioned genes involved in lipogenesis (Fig. 3B and Supplemental Fig. 3B). Both concurrent and post-treatment with CA significantly decreased the mRNA message of glycerol-3-phosphate acyltransferase 1 mitochondrial (GPAM), glycerol-3-phosphate acyltransferase 2 (GPAT2), diacyl glycerol acyl transferase 2 (DGAT2), and monoacylglycerol O-acyltransferase 1 (MOGAT1) that are associated with triglyceride synthesis (Fig. 3C and Supplemental Fig. 3C). Simultaneous CA and PA/OA treatment as well as CA treatment after PA administration also reduced expression of diacyl glycerol acyl transferase 1 (DGAT1), a critical enzyme responsible for the conversion of diacylglycerols to

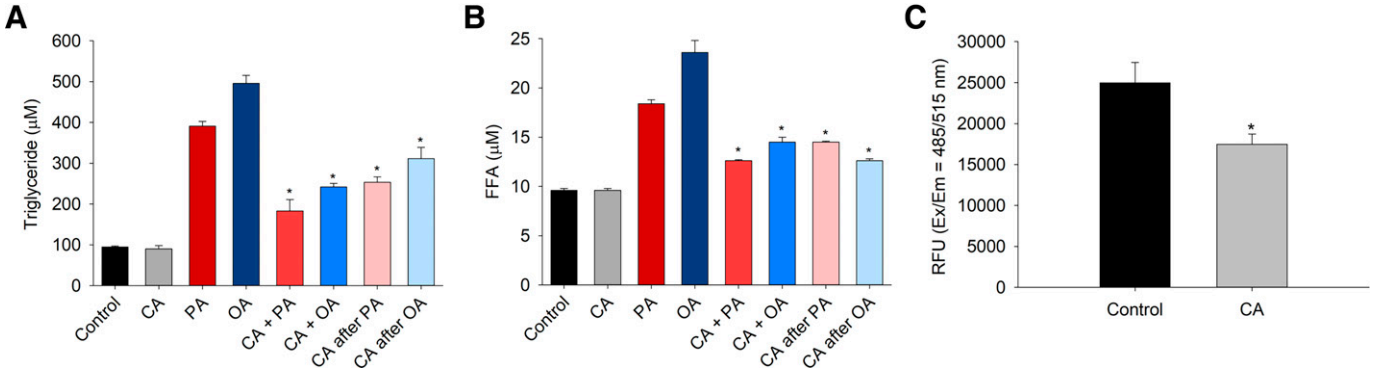

Fig. 2. Quantification of (A) triglyceride, (B) free fatty acid content, and (C) free fatty acid uptake in HepG2 cells treated with 500-μM BSA + DMSO (control), 30-μM CA, 500-μM PA, 500-μM OA, 30-μM CA+ 500-μM PA/OA, 30-μM CA after 500-μM PA/OA. Triglyceride content was measured using a luminescence assay, whereas free fatty acid content and free fatty acid uptake were determined fluorometrically. Data are represented as mean ± SD ($n = 3$). *$P < 0.05$ compared with PA/OA-only treatment group.

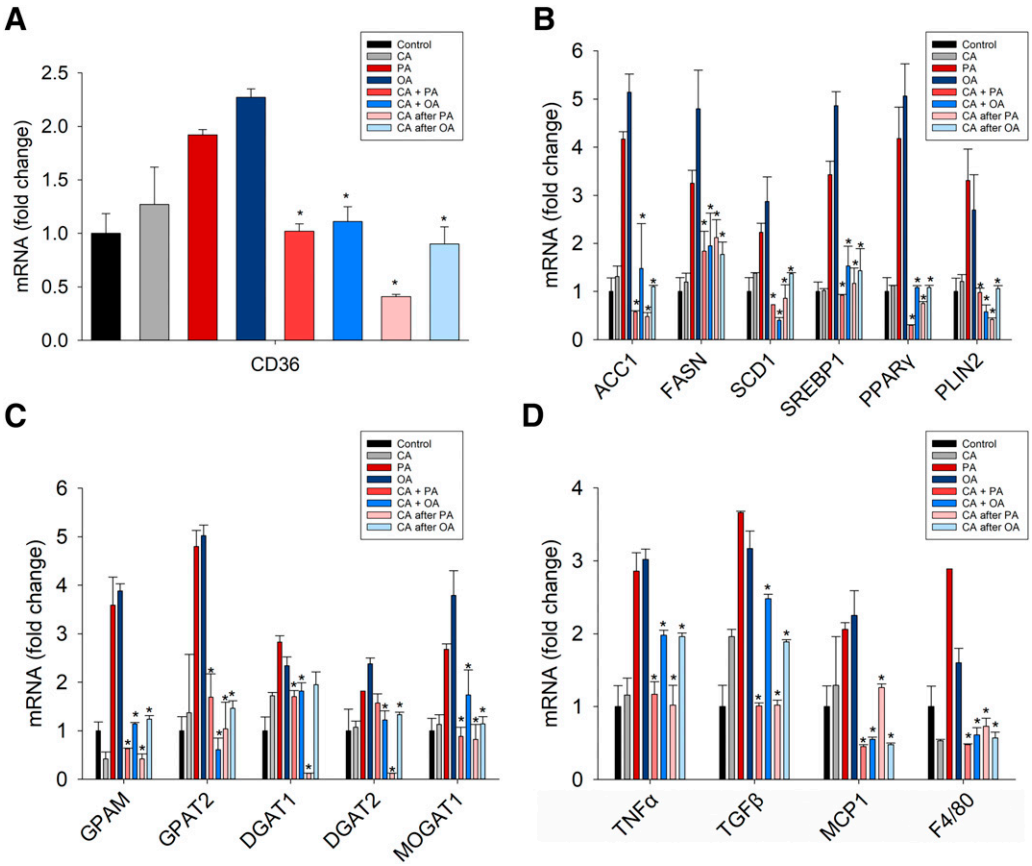

Fig. 3. Expression of mRNAs encoding genes involved in (A) free fatty acid transport, (B) fatty acid synthesis, (C) triglyceride synthesis, and (D) inflammation. HepG2 cells were treated with 500-μM BSA+ DMSO (control), 30-μM CA, 500-μM PA, 500-μM OA, 30-μM CA+ 500-μM PA/OA, 30-μM CA after 500-μM PA/OA. mRNA message was analyzed by qRT-PCR and normalized to 18S rRNA. Results are expressed as fold of the value found in control treatment arbitrarily set at 1. For statistical analysis, a mixed-effects multivariate ANOVA (MANOVA) model was used. After an overall significant F test from MANOVA model, the post hoc multiple-comparison tests were performed for the pre-specified comparisons adjusted by Tukey procedure. Data are represented as mean ± SD ($n = 3$). *$P < 0.05$ compared with PA/OA-only treatment group.

triglycerides (Fig. 3C and Supplemental Fig. 3C). Expression of markers of inflammation and pro-inflammatory cytokines, including tumor necrosis factor alpha (TNFα), transforming growth factor beta (TGFβ), monocyte chemoattractant protein (MCP1), and monocyte-macrophage marker F4/80, were suppressed in response to CA treatment (Fig. 3D and Supplemental Fig. 3D). Our results thus highlight the role of CA in averting the NAFLD pathology in an in vitro model by reducing the uptake, synthesis, and deposition of lipids, and curbing the inflammatory responses.

CA Treatment Reduces Body Mass Gain in High-Fat-Diet Fed Mice. We next evaluated the potential of CA to protect against an in vivo high-fat-diet induced model of non-alcoholic fatty liver disease. Mice were fed a control diet (CD), high-fat diet (HFD), HFD with CA administration for 16 weeks (CA + HFD), and HFD for 16 weeks with CA-regimen starting from week 10 (CA after HFD). As expected, the HFD-fed mice gained significantly higher body mass than CD-fed mice. Treatment with CA reduced the weight gain in both CA + HFD and CA after HFD groups (Fig. 4, A–C). Mice in the CA + HFD group displayed significant loss of weight gain after 9 weeks of CA treatment. The body mass gain of mice in the CA after HFD group was similar to that of the HFD group until week nine, but started to decline after CA administration from week 10 with significant reduction in body mass from week 14 (Fig. 4, B and C). The liver weight and liver weight normalized to total body weight was reduced significantly in CA-treated mice (Fig. 4, D and E). Finally, the reduction in weight gain upon CA treatment was not attributed to caloric consumption as there were no differences in dietary intake between various groups (Fig. 4F).

CA Alleviates Steatosis and Hepatic Injury As Well As Improves Glucose Metabolism. Long-term high-fat-diet feeding is known to induce metabolic disturbances and macrovascular steatosis. Therefore, we examined the role of CA in regulating hepatic lipid deposition. Histopathological analysis revealed that HFD-fed mice developed severe steatosis compared with the CD-fed mice, while treatment with CA mitigated the lipid accumulation in the liver (Fig. 5A). Moreover, the CA regimen resulted in the reduction of hepatic triglyceride and cholesterol content (Fig. 5, B and C). Serum ALT assays confirmed that the liver injury induced by the high-fat diet was attenuated with CA treatment (Fig. 5D). These data confirmed that CA exerts anti-steatotic and cytoprotective effects against high-fat-diet–induced lipotoxicity. Hepatic steatosis is connected with impaired glucose metabolism, therefore we measured blood glucose levels and conducted an oral glucose tolerance test (Ochi et al., 2017). CA treatment significantly lowered the fasting blood glucose levels (Fig. 6A) and improved glucose tolerance (Fig. 6, B and C) indicating recuperation from metabolic deterioration.

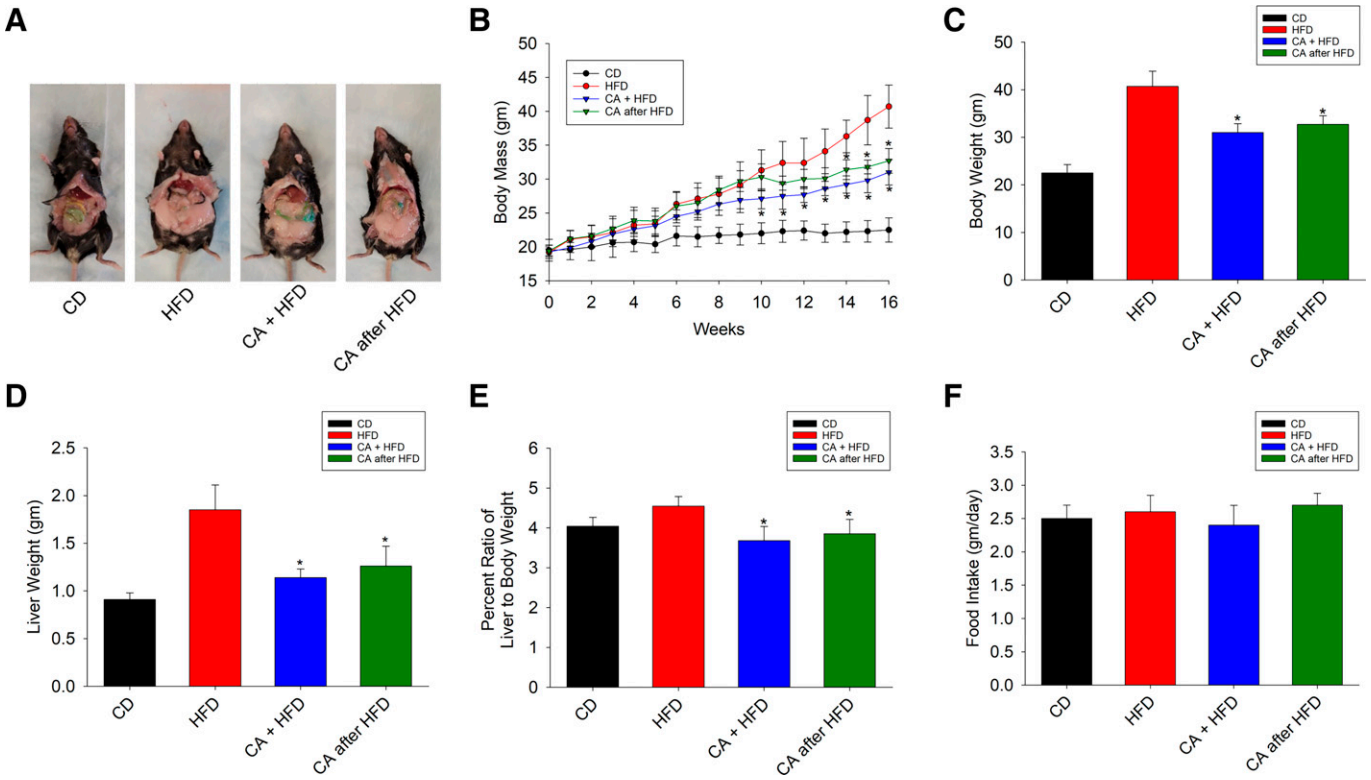

Fig. 4. CA treatment reduces body and liver weight of high-fat-diet fed mice. C57BL6 mice were fed with a control diet (CD) for 16 weeks, high-fat diet (HFD) for 16 weeks, high-fat diet and treated with CA for 16 weeks (CA + HFD), and high-fat diet for 16 weeks with CA treatment initiated after 10 weeks of exposure to HFD for a remaining 6 weeks (CA after HFD). (A) Representative image of mice after 16 weeks of diet, (B) body mass, (C) body weight at the end of the study, week 16, (D) weight of the liver at week 16, (E) percentage ratio of liver weight normalized to total body weight at the end of the study, and (F) daily food intake calculated from the average of weekly food intake. Data are represented as mean ± SD ($n = 7$). *$P < 0.05$ compared with HFD-only treatment group.

CA Regulates Lipid Metabolism In Vivo. To obtain mechanistic insight by which CA mitigates hepatic lipid accumulation, several key genes regulating fatty acid uptake and metabolism were examined. Both CA + HFD and CA after HFD treatments resulted in the significant downregulation of CD36, which facilitates hepatic uptake of long-chain fatty acids (Fig. 7A). Correspondingly, several critical genes regulating lipid synthesis that were upregulated under HFD-fed

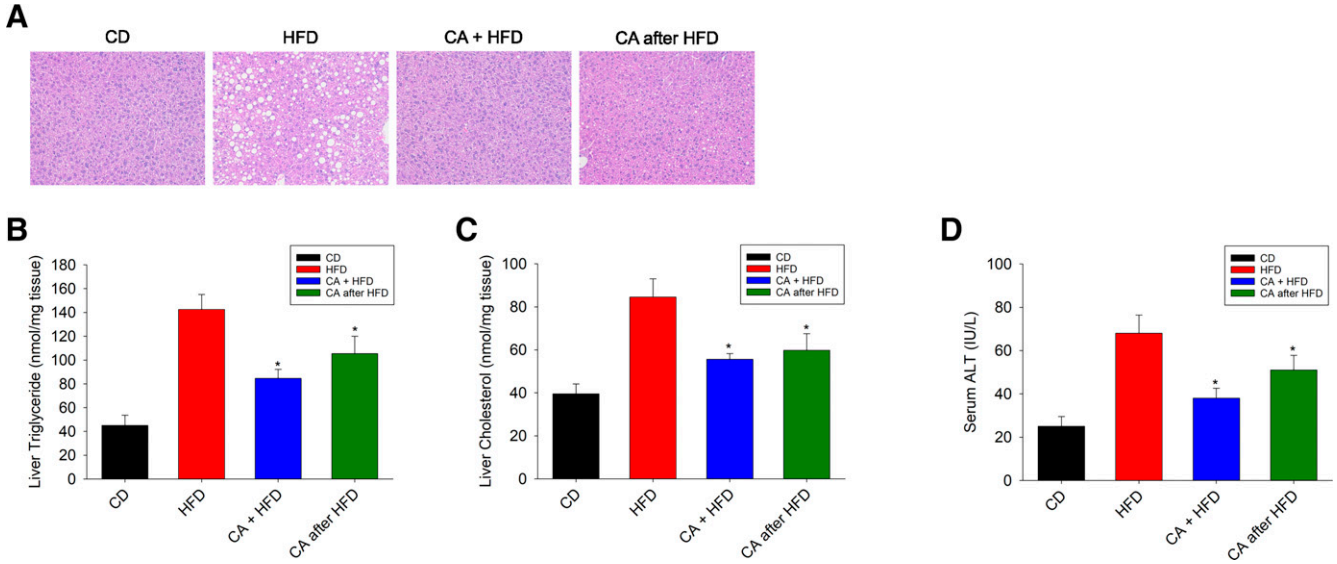

Fig. 5. CA alleviates steatosis and hepatic injury in high-fat-diet fed mice. (A) Representative image of H&E-stained liver sections, (B) liver triglycerides, (C) liver cholesterol, and (D) serum ALT measurement of mice fed with control diet (CD) for 16 weeks, high fat diet (HFD) for 16 weeks, high-fat diet and treated with CA for 16 weeks (CA + HFD), and high-fat diet for 16 weeks with CA treatment initiated after 10 weeks of exposure to HFD for remaining 6 weeks (CA after HFD). Data are represented as mean ± SD ($n = 7$). *$P < 0.05$ compared with HFD-only treatment group.

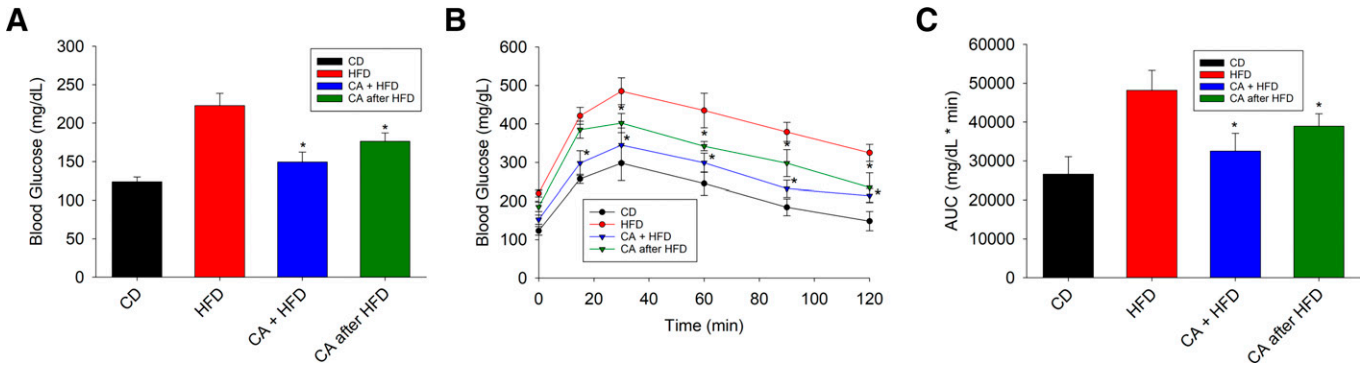

Fig. 6. CA lowers blood glucose levels and improves glucose tolerance in HFD-fed mice. Mice were fed with control diet (CD), high-fat diet (HFD), high-fat diet with CA treatment (CA + HFD) for 16 weeks, and with high-fat diet for 16 weeks with CA treatment initiated after 10 weeks of HFD feeding for the last 6 weeks (CA after HFD). (A) Fasting blood glucose measurement, (B) glucose tolerance test performed, and (C) the area under the curve calculated for respective groups. Data are represented as mean ± SD ($n = 7$). *$P < 0.05$ compared with HFD-only treatment group.

conditions showed a significant decrease after CA treatment (Fig. 7, B and C). Treatment with CA significantly upregulated liver mRNA levels of mitochondrial beta oxidation genes, carnitine palmitoyl transferase 1a (CPT1a), and carnitine palmitoyl transferase 2 (CPT2). However, no change in the expression of acyl-CoA oxidase1 (ACOX1), a marker of peroxisomal oxidation, was seen (Fig. 7D). CA administration mitigated inflammatory response as observed by the downregulation of the expression of the inflammatory markers (Fig. 7E). Collectively, our data suggest that CA treatment regulates free fatty uptake and attenuates de novo lipogenesis thereby ameliorating steatosis observed in NAFLD.

CA-Induced Steatoprotection Is Dependent on AhR-Driven Stc2 Signaling. CA is a known AhR agonist that specifically induces hepatic expression of an AhR target gene, Stc2, without Cyp1a1 upregulation (Patil et al., 2022). In HFD-fed mice livers, Stc2 expression was downregulated (Supplemental Fig. 4A). Upon CA treatment, AhR directly interacted with the Stc2 promoter region containing 8 xenobiotic response elements resulting in a significant induction of Stc2 without Cyp1a1 upregulation (Supplemental Fig. 4, A and C) (Harper et al., 2013; Joshi et al., 2015). Moreover, CA treatment resulted in Stc2 upregulation in vitro, indicating activation of an AhR signaling cascade (Supplemental Fig. 4B). Knowing that the CA-induced AhR-mediated Stc2 expression is critical for the protection against a plethora of endoplasmic reticulum/oxidative stressors (Joshi et al., 2015), we investigated whether the anti-steatotic effects of CA are mediated by AhR-Stc2 signaling. First, the role of AhR in CA-mediated protection was interrogated by silencing AhR in HepG2 cells. HepG2 cells were transiently transfected with AhR siRNA and non-targeting (scrambled) oligonucleotides. AhR expression was suppressed with RNA interference and confirmed by Western blotting (Fig. 8A). Using histology, we analyzed the degree of steatosis in AhR-silenced OA-treated HepG2 cells in the presence and absence of CA. CA treatment failed to provide protection against OA-induced steatosis in AhR knocked-down cells, whereas in AhR-positive cells (non-targeting siRNA treated), CA markedly attenuated accumulation of intracellular lipids (Fig. 8B). Subsequent quantitation of triglycerides and free fatty acids in AhR-silenced PA/OA- treated HepG2 cells indicated no effect of CA treatment (Fig. 8, C and D). In contrast, control HepG2 cells treated with CA reduced both triglycerides and free fatty acid content (Fig. 2, A and B). Suppressing AhR in HepG2 cells elevated long-chain fatty acid uptake compared with untransfected (control) and nontargeting siRNA treated cells. CA treatment did not attenuate free fatty acid uptake in AhR-silenced HepG2 cells, but was able to mitigate fatty acid uptake in control and non-targeting siRNA treated cells (Fig. 8E). We further investigated if silencing AhR in HepG2 cells had any effect on the expression of genes associated with lipid metabolism and inflammation when induced with PA/OA and treated simultaneously, or after 24 hours, with CA. In the absence of AhR, CA treatment did not downregulate genes involved in fatty acid uptake (CD36), fatty acid synthesis (ACC1, FASN, SREBP1, PPARγ), triglyceride synthesis (GPAM, GPAT2, DGAT1, DGAT2, MOGAT1), and inflammation (TNFα, TGFβ, MCP1, F4/80) (Fig. 8, F–I). To further investigate the potential function of the AhR target gene, Stc2 in CA-induced, AhR-driven protection against lipotoxicity, Stc2 expression in HepG2 cells was knocked-down using RNA interference (Fig. 9A). In the absence of Stc2, CA did not protect against steatosis (Fig. 9B), or mitigated triglyceride, fatty acid accumulation, and hepatic uptake of free fatty acids (Fig. 9, C–E). Moreover, in Stc2 silenced cells, CA treatment failed to attenuate expression of fatty acid uptake, lipid synthesis, and inflammation markers (Fig. 9, F–I). Therefore, the findings presented here strongly indicate that the anti-steatotic and hepatoprotective effects against lipotoxicity exerted by CA are absolutely dependent upon AhR-mediated Stc2 signaling.

Discussion

Non-alcoholic fatty liver disease is a liver manifestation of metabolic syndrome in the absence of alcohol intake. It covers an array of pathologic conditions ranging from steatosis to complex hepatocellular injury, inflammation, and fibrosis (non-alcoholic steatohepatitis, NASH). The global epidemic of NAFLD, the number one hepatic disease worldwide, is rapidly increasing owing to growing prevalence of obesity and type 2 diabetes mellitus. In the United States, NAFLD affects approximately 85 million adults and 8 million children, and currently is the second most common cause of liver transplantation (Shetty and Syn, 2019). Currently, lifestyle changes in diet and exercise are shown to be the most effective interventions against NAFLD (Fernández et al., 2022). Additionally, The American Association for the Study of Liver Diseases

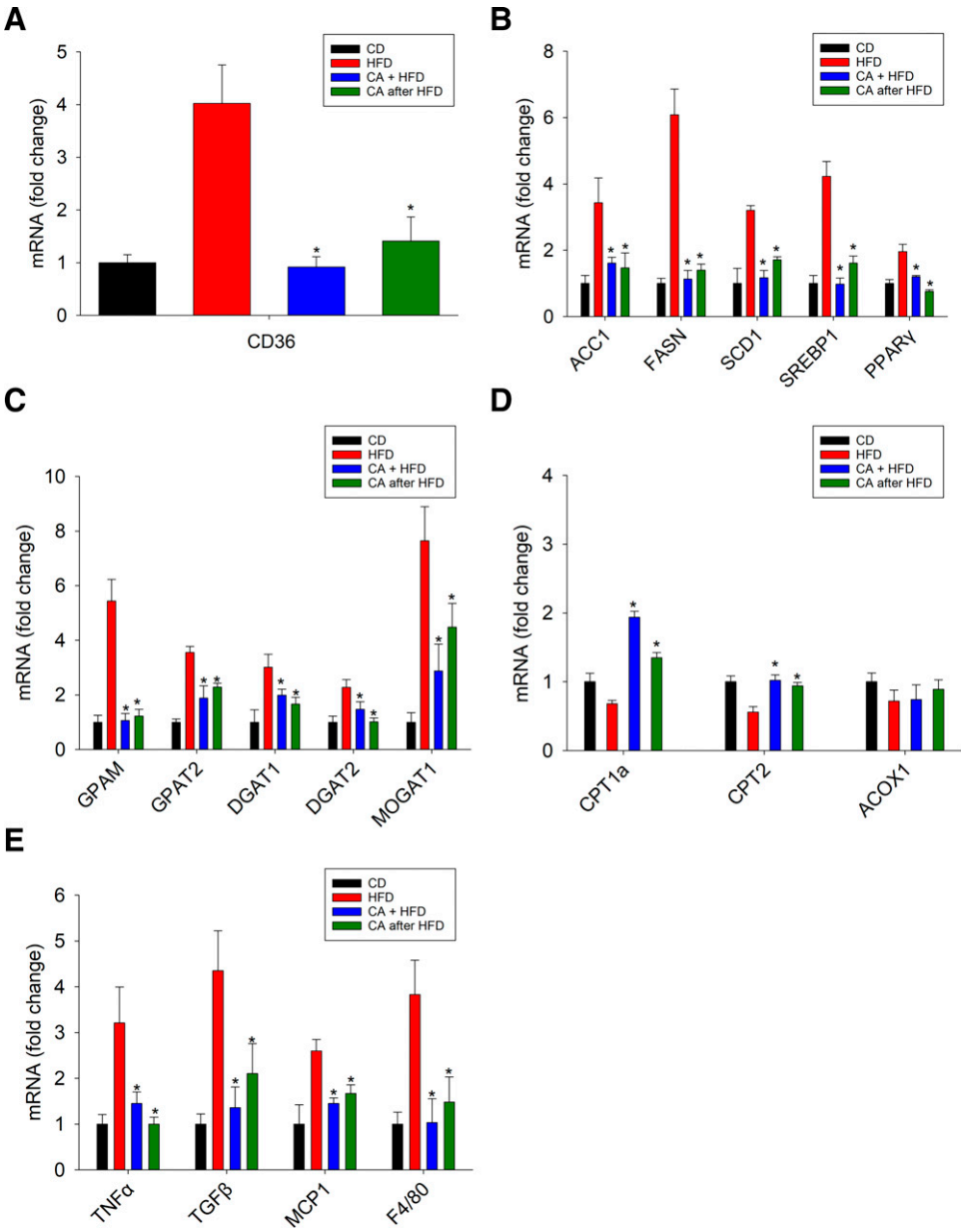

Fig. 7. CA attenuates hepatic free fatty acid uptake, lipogenesis, and inflammation in vivo. C57BL6 mice were fed with a control diet (CD) for 16 weeks, high-fat diet (HFD) for 16 weeks, high-fat diet and CA treatment for 16 weeks (CA + HFD), and high-fat diet for 16 weeks with CA treatment for last 6 weeks (CA after HFD). mRNA expression of markers for (A) free fatty acid transport, (B) de novo lipogenesis, (C) triglyceride synthesis, (D) fatty acid oxidation, and (E) inflammation, were analyzed by qRT-PCR and normalized to 18S rRNA. Results are expressed as fold of the value found in control treatment arbitrarily set at 1. Data are represented as mean ± SD ($n = 7$). *$P < 0.05$ compared with HFD-only treatment group.

guidelines recommend the use of off-label piaglitazone, a PPARγ agonist and vitamin E, for biopsy-proven NASH adult patients only after discussing and considering the risks and benefits (Zhang and Yang, 2021). With the absence of Food and Drug Administration approved treatments, characterization of unmined pathways and identification of novel future therapeutics is warranted.

Cinnabarinic acid, a tryptophan metabolite and a byproduct of the kynurenine pathway is shown to be an endogenous agonist for AhR (Lowe et al., 2014). Taking advantage of a cre-lox system to manipulate the status of AhR, our previous study identified Stc2 as a novel receptor target gene (Harper et al., 2013). These findings were important as a CA treatment-induced expression of Stc2 in an AhR-dependent manner, and failed to upregulate expression of the archetypical AhR target gene, Cyp1a1, in the liver (Joshi et al., 2015). Very few studies have investigated the therapeutic potential of CA. CA protected against endoplasmic reticulum/oxidative stress-induced apoptosis in isolated primary hepatocytes (Joshi et al., 2015). Moreover, CA conferred protection against steatosis, apoptosis, and hepatic injury in an acute and NIAAA chronic plus binge model of alcoholic liver disease, in an AhR- and Stc2-dependent manner (Joshi et al., 2015; Joshi et al., 2022). In an experimental model of multiple sclerosis in mice, daily CA injections (0.1 – 10 mg/kg) protected against autoimmune encephalomyelitis (Fazio et al., 2014). In

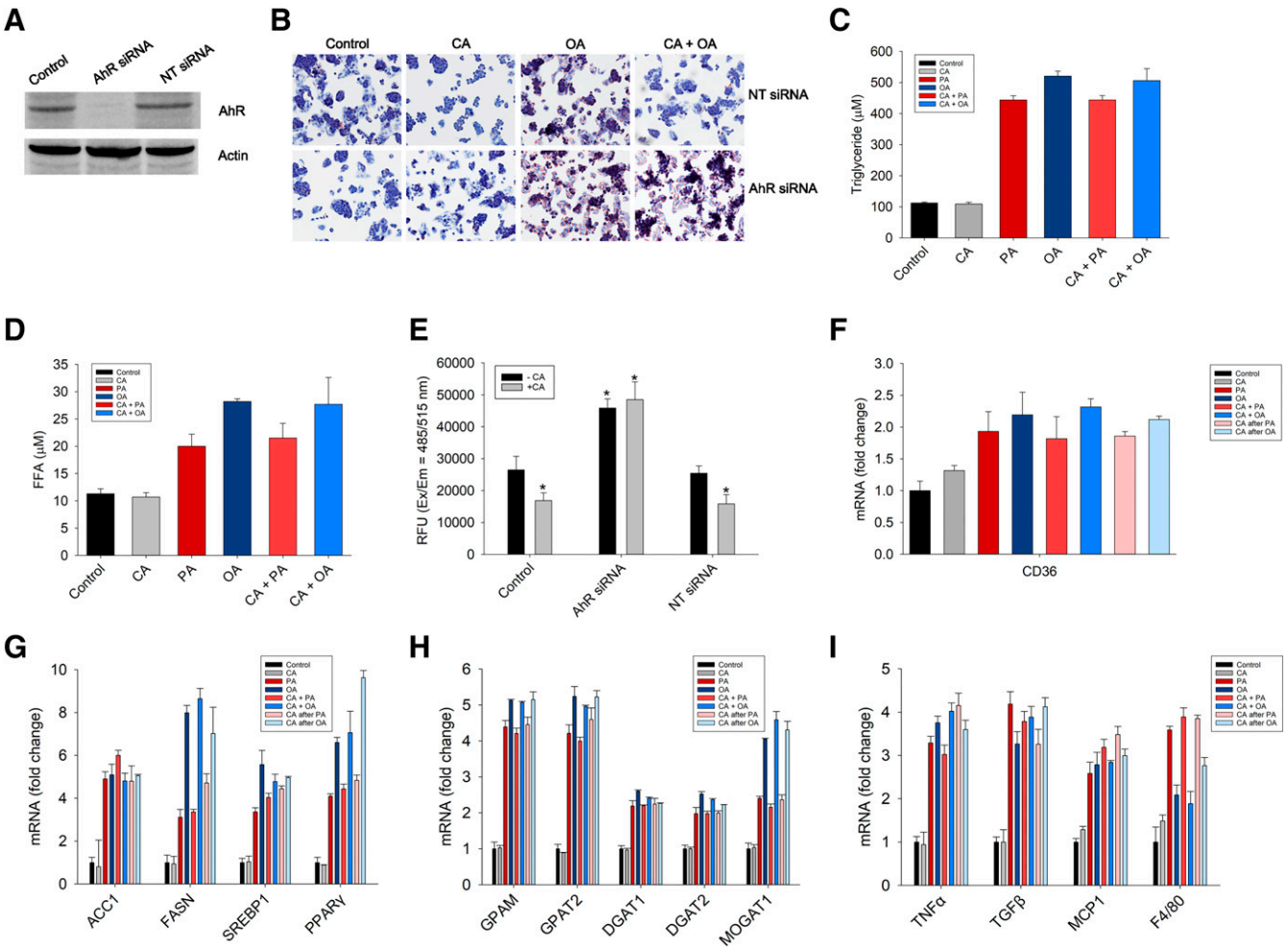

Fig. 8. CA failed to protect against NAFLD in an AhR-silenced in vitro model. HepG2 cells were transiently transfected with AhR or non-targeting (scrambled) siRNA for 24 hours followed by 500-μM BSA+ DMSO (control), 30-μM CA, 500-μM PA, 500-μM OA, 30-μM CA+ 500-μM PA, 30-μM CA+ 500-μM OA and/or 30-μM CA 24 hours after 500-μM PA/OA treatments. (A) Western blotting on total lysate was performed to monitor AhR expression. Actin was probed as a control. (B) Oil red O staining to detect lipid content. Quantification of (C) triglyceride. (D) Free fatty acid content. (E) Free fatty acid uptake; mRNA expression of genes involved in (F) free fatty acid uptake. (G) Fatty acid synthesis. (H) Triglyceride synthesis. (I) Inflammation, normalized to 18S rRNA. Data are represented as mean ± SD ($n = 3$). *$P < 0.05$ compared with an untransfected control group not treated with CA.

mice, basal concentration of CA is ≈ 400 pg/ml and ≈ 10 pg/mg in serum and liver, respectively. A daily 12 mg/kg CA i.p. regimen elevated CA concentration in serum to ≈ 6000 pg/ml and resulted in a 50% increase in liver CA concentration (≈ 15 pg/mg) (Joshi et al., 2022). Our in vivo studies have observed activation of AhR and upregulation of Stc2 within 2 hours of 12 mg/kg CA treatment (Patil et al., 2022), and a daily CA administration was able to maintain an elevated Stc2 expression (Supplemental Fig. 4, A and C) (Joshi et al., 2022). These observations indicate that from a clinically relevant therapeutic perspective, a pharmacotherapeutic formulation or dietary supplementation of CA will be essential for activating AhR-Stc2 mediated hepatoprotective signaling pathways. A recent study indicated the half-life of CA to be 4 hours in isolated rat liver microsomes (Gómez-Piñeiro et al., 2022); therefore future studies will need to be performed to comprehensively examine the mechanism of CA production within the endogenous tryptophan metabolism pathway, and determine in vivo stability of CA.

Selection and specificity of AhR agonists, ligand-induced conformational changes in AhR recruiting various enhancing/inhibitory cofactors, specific post-translational modifications responsible for promoter modulation, and subsequent signaling pathways contribute toward the potential detrimental or beneficial function of AhR in NAFLD (Safe et al., 2018; Murray and Perdew, 2020; Carambia and Schuran, 2021). The TCDD regimen resulted in an AhR-mediated upregulation of the fibrogenic pathway and development of liver fibrosis (Pierre et al., 2014). An activation of AhR with Benzo[a]pyrene promoted fatty liver disease (Zhu et al., 2020), whereas administration of an AhR antagonist, α-naphthoflavone, attenuated hallmarks of NAFLD (Xia et al., 2019). Therefore, in response to various exogenous ligands, AhR has been implicated to promote NAFLD by regulating the expression of target genes including CD36, CYP1A1, TNF-α, and Fibroblast growth factor 21 (FGF21) (Walisser et al., 2005; Lee et al., 2010; Xia et al., 2019; Zhu et al., 2020). On the contrary, a protective role of AhR in NAFLD has also been documented. Loss of AhR has shown to cause multiple physiologic abnormalities including an accelerated rate of apoptosis, decreased liver size, and liver fibrosis around the portal triad (Fernandez-Salguero et al., 1995). Recently, a hepatocyte-specific AhR knockout

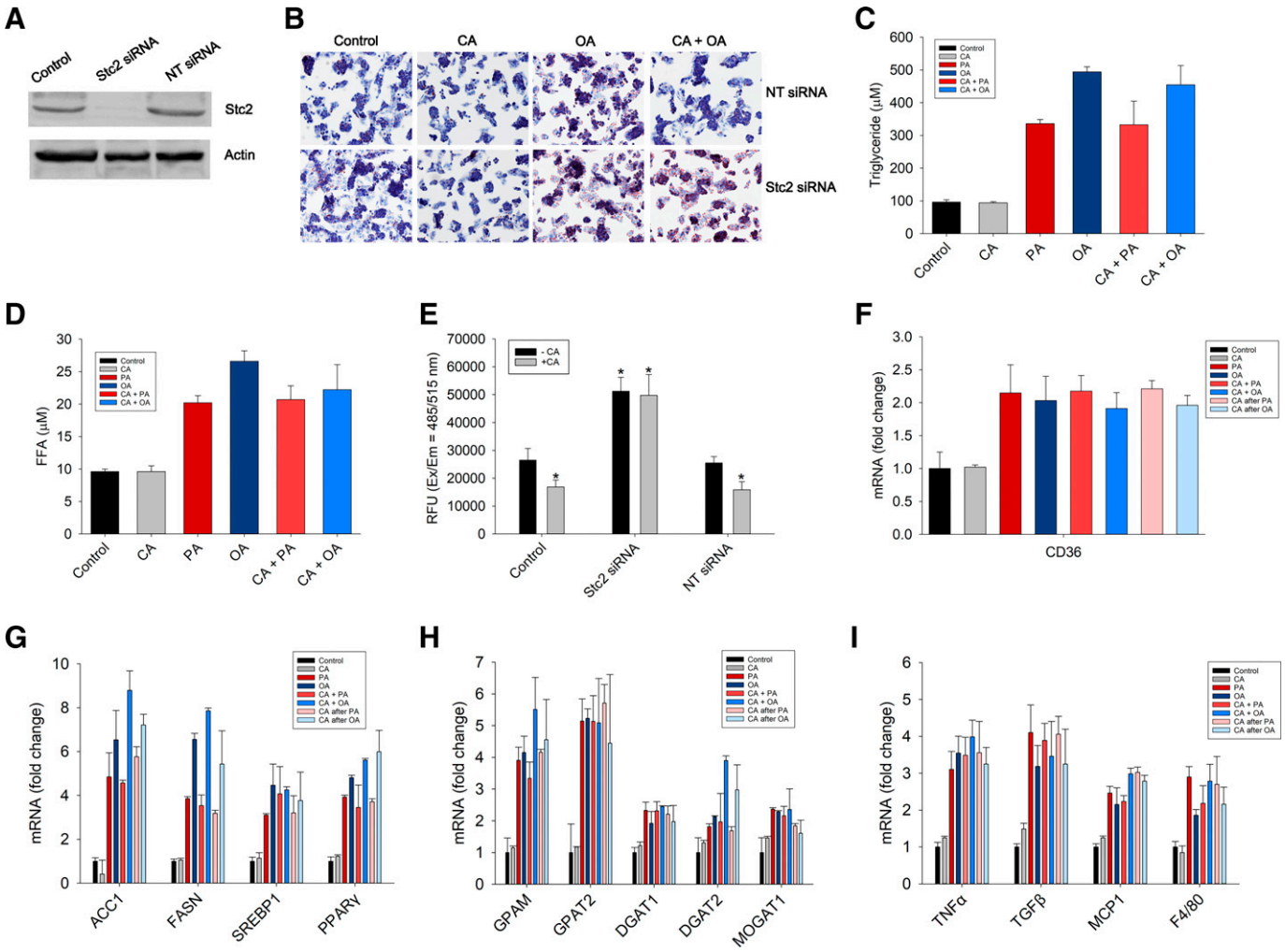

Fig. 9. CA-mediated protection against lipotoxicity is Stc2 dependent. HepG2 cells were transiently transfected with Stc2 or non-targeting (scrambled) siRNA for 24 hours followed by 500-μM BSA+ DMSO (control), 30-μM CA, 500-μM PA, 500-μM OA, 30-μM CA+ 500-μM PA, 30-μM CA+ 500-μM OA and/or 30-μM CA 24 hours after 500-μM PA/OA treatments. (A) Stc2 expression in total lysate was monitored by performing immunoblotting. Actin was used as a control. (B) Lipid content was detected using oil red O staining. Quantification of (C) triglyceride, (D) free fatty acid, and (E) free fatty acid uptake. Expression of genes involved in (F) free fatty acid uptake, (G) fatty acid synthesis, (H) triglyceride synthesis, and (I) inflammation, was quantitated by performing quantitative RT-PCR, normalized to 18S rRNA. Data are represented as mean ± SD (n = 3). *$P < 0.05$ compared with an untransfected control group untreated with CA.

mouse model indicated AhR's protective role against high-fat-diet induced hepatic steatosis and lipotoxicity by regulation of the Socs3 gene (Wada et al., 2016). A gut-microbiota-derived tryptophan metabolite mitigated fatty acid induced inflammation and lipogenesis in hepatocytes – and the effects were AhR-dependent (Krishnan et al., 2018). Similarly, microbiota-derived endogenous AhR ligands, indole-3-acetic acid and indole, were able to attenuate steatosis in NAFLD (Hendrikx and Schnabl, 2019; Ji et al., 2019). CA, unlike prototypical AhR agonists, does not induce Cyp1a1 expression, but upregulates expression of Stc2. Hepatic Stc2 expression was shown to be reduced in both obese (ob/ob) and high-fat-diet fed mice, and the recombinant Stc2 administration downregulated expression of lipogenic genes and ameliorated hepatosteatosis (Jiao et al., 2017; Zhao et al., 2018). Therefore, it is conceivable that CA-induced AhR-mediated Stc2 upregulation activates anti-steatotic signaling to alleviate hepatic steatosis and inflammation in vitro. It is also plausible that other AhR target genes, cross-talking transcription factors, and signaling pathways, including TLR4 (Liu et al., 2014), SREBP1 (Krishnan et al., 2018; Muku et al., 2019), estrogen signaling (Zhu et al., 2020), SOCS3 (Wada et al., 2016), and NF-kB (Zeng et al., 2014; Larigot et al., 2018), are involved in protection – albeit the exact mechanism of CA-mediated AhR-Stc2–dependent hepatoprotection in vivo is uncharacterized and future studies investigating the mechanism of protection against lipotoxicity are warranted.

The early stage of NAFLD is primarily characterized by excessive lipid accumulation in hepatocytes. This study was successful in mimicking the first stage of NAFLD pathology in vitro using palmitic acid and oleic acid (major free fatty acids found in NAFLD patients), and in vivo by feeding mice a high-fat diet (60 kcal%) – as evidenced by the aggregation of a large number of lipid droplets in hepatic cell lines (Fig. 1B), macrovascular steatosis in mice livers (Fig. 5A), and an increase in triglyceride and cholesterol (Fig. 5, B and C). However, treatment with CA significantly prevented weight gain (Fig. 4, A–C), attenuated steatosis (Figs. 1B and 5A), and mitigated metabolic deterioration, as seen by lowered fasting glucose and improved glucose tolerance (Fig. 6), suppressed

inflammation due to high-fat-diet feeding (Fig. 7E), and protected against hepatic injury (Fig. 5D). We identified that CA treatment downregulated the expression of fatty acid translocase, CD36 (Fig. 3A), concomitantly with a decrease in hepatic free fatty acid uptake (Fig. 2C). NAFLD patients have abnormally high levels of CD36 which positively correlates with the histologic grade of hepatic steatosis (Rada et al., 2020), whereas hepatocyte specific knockout of CD36 attenuated fatty liver disease and improved insulin sensitivity in high-fat-diet fed mice (Wilson et al., 2016). Therefore, it is conceivable that CA regulates hepatic CD36-mediated uptake of long-chain fatty acids and alleviates hepatosteatosis. The reduced weight gain, without a change in food intake, suggests that CA may act on other tissues in addition to the liver and that the reduction of CD36 may not be unique to the liver. Therefore in the future it will be important to determine whether CA alters adipose tissue thermogenesis and/or fatty acid uptake by gut (Rada et al., 2020). We did not observe significant changes in other fatty acid transporters, including fatty acid transport protein 2 (FATP2), in response to CA treatment (data not shown). Both in vitro and in vivo studies showed that CA treatment after the onset of steatosis was able to mitigate metabolic deterioration and steatohepatitis. These data strongly suggest that the reversal of steatosis occurs by not only hindering lipogenesis, but also via the potential increase in the rate of mitochondrial fatty acid oxidation, and/or transport of triglycerides to other tissues, including muscles and adipose. Accordingly, we identified the elevation of a rate-determining enzyme for mitochondrial beta-oxidation, CPT1a, in response to CA treatment. However, the marker of peroxisomal beta-oxidation, ACOX1, was unaltered (Xu et al., 2021). Therefore, it is plausible that CA treatment preferentially activates hepatic mitochondrial oxidation and contributes to mitigating NAFLD, although whether CA stimulates a SIRT1-PGC1α signaling cascade needs to be determined. Further studies beyond the scope of this manuscript will also investigate the mechanism by which CA-induced AhR-Stc2 signaling regulates specific lipid metabolism pathways and alleviates steatosis.

The findings of this study confirmed that CA bestowed hepatic protection in both in vitro and in vivo NAFLD models by suppressing hepatic free fatty acid uptake and regulating genes involved in lipid metabolism. CA improved glucose tolerance, dampened the expression of pro-inflammatory cytokines that exacerbate NAFLD pathology, and protected against hepatic steatosis and injury. Moreover, CA-mediated hepatoprotection against fatty liver pathology was contingent upon AhR-mediated Stc2 expression. In summary, the identification of the hepatoprotective function of the endogenous AhR agonist, CA will be instrumental in the development of future novel therapeutic interventions against metabolic liver diseases.

Authorship Contributions

Participated in research design: Patil, Mandala, Friedman, Joshi.

Conducted experiments: Patil, Rus, Downing.

Contributed new reagents or analytic tools: Patil, Mandala.

Performed data analysis: Patil, Joshi.

Wrote or contributed to the writing of the manuscript: Patil, Rus, Downing, Friedman, Mandala, Joshi.

References

Angulo P (2002) Nonalcoholic fatty liver disease. *N Engl J Med* **346**:1221–1231.

Bugianesi E, Leone N, Vanni E, Marchesini G, Brunello F, Carucci P, Musso A, De Paolis P, Capussotti L, Salizzoni M et al. (2002) Expanding the natural history of nonalcoholic steatohepatitis: from cryptogenic cirrhosis to hepatocellular carcinoma. *Gastroenterology* **123**:134–140.

Carambia A and Schuran FA. (2021) The aryl hydrocarbon receptor in liver inflammation. *Semin Immunopathol* **43**:563–575.

Cobbina E and Akhlaghi F (2017) Non-alcoholic fatty liver disease (NAFLD) - pathogenesis, classification, and effect on drug metabolizing enzymes and transporters. *Drug Metab Rev* **49**:197–211.

Cohen JC, Horton JD, and Hobbs HH (2011) Human fatty liver disease: old questions and new insights. *Science* **332**:1519–1523.

Day CP and James OF (1998) Steatohepatitis: a tale of two "hits"? *Gastroenterology* **114**:842–845.

de Alwis NMW and Day CP (2008) Non-alcoholic fatty liver disease: the mist gradually clears. *J Hepatol* **48** (Suppl 1):S104–S112.

Denison MS and Nagy SR (2003) Activation of the aryl hydrocarbon receptor by structurally diverse exogenous and endogenous chemicals. *Annu Rev Pharmacol Toxicol* **43**:309–334.

Farrell GC and Larter CZ (2006) Nonalcoholic fatty liver disease: from steatosis to cirrhosis. *Hepatology* **43**(2, Suppl 1)S99–S112.

Faul F, Erdfelder E, Buchner A, and Lang AG (2009) Statistical power analyses using G*Power 3.1: tests for correlation and regression analyses. *Behav Res Methods* **41**:1149–1160.

Fazio F, Zappulla C, Notartomaso S, Busceti C, Bessede A, Scarselli P, Vacca C, Gargaro M, Volpi C, Allegrucci M et al. (2014) Cinnabarinic acid, an endogenous agonist of type-4 metabotropic glutamate receptor, suppresses experimental autoimmune encephalomyelitis in mice. *Neuropharmacology* **81**:237–243.

Fernández T, Viñuela M, Vidal C, and Barrera F (2022) Lifestyle changes in patients with non-alcoholic fatty liver disease: A systematic review and meta-analysis. *PLoS One* **17**:e0263931.

Fernandez-Salguero P, Pineau T, Hilbert DM, McPhail T, Lee SS, Kimura S, Nebert DW, Rudikoff S, Ward JM, and Gonzalez FJ (1995) Immune system impairment and hepatic fibrosis in mice lacking the dioxin-binding Ah receptor. *Science* **268**: 722–726.

Friedman SL, Neuschwander-Tetri BA, Rinella M, and Sanyal AJ (2018) Mechanisms of NAFLD development and therapeutic strategies. *Nat Med* **24**:908–922.

Gómez-Piñeiro RJ, Dali M, Mansuy D, and Boucher JL (2022) Unstability of cinnabarinic acid, an endogenous metabolite of tryptophan, under situations mimicking physiological conditions. *Biochimie* **199**:150–157.

Guo L, Kang JS, Park YH, Je BI, Lee YJ, Kang NJ, Park SY, Hwang DY, and Choi YW (2020) S-petasin inhibits lipid accumulation in oleic acid-induced HepG2 cells through activation of the AMPK signaling pathway. *Food Funct* **11**:5664–5673.

Harper Jr TA, Joshi AD, and Elferink CJ (2013) Identification of stanniocalcin 2 as a novel aryl hydrocarbon receptor target gene. *J Pharmacol Exp Ther* **344**:579–588.

Hendrikx T and Schnabl B (2019) Indoles: metabolites produced by intestinal bacteria capable of controlling liver disease manifestation. *J Intern Med* **286**:32–40.

Ipsen DH, Lykkesfeldt J, and Tveden-Nyborg P (2018) Molecular mechanisms of hepatic lipid accumulation in non-alcoholic fatty liver disease. *Cell Mol Life Sci* **75**:3313–3327.

Ji Y, Gao Y, Chen H, Yin Y, and Zhang W (2019) Indole-3-acetic acid alleviates nonalcoholic fatty liver disease in mice via attenuation of hepatic lipogenesis, and oxidative and inflammatory stress. *Nutrients* **11**:2062.

Jiao Y, Zhao J, Shi G, Liu X, Xiong X, Li X, Zhang H, Ma Q, and Lu Y (2017) Stanniocalcin2 acts as an anorectic factor through activation of STAT3 pathway. *Oncotarget* **8**:91067–91075.

Joshi AD, Thinakaran G, and Elferink C (2022) Cinnabarinic acid-induced stanniocalcin 2 confers cytoprotection against alcohol-induced liver injury. *J Pharmacol Exp Ther* **381**:1–11.

Joshi AD (2020) New insights into physiological and pathophysiological functions of stanniocalcin 2. *Front Endocrinol (Lausanne)* **11**:172.

Joshi AD, Carter DE, Harper Jr TA, and Elferink CJ (2015) Aryl hydrocarbon receptor-dependent stanniocalcin 2 induction by cinnabarinic acid provides cytoprotection against endoplasmic reticulum and oxidative stress. *J Pharmacol Exp Ther* **353**:201–212.

Kawano Y and Cohen DE (2013) Mechanisms of hepatic triglyceride accumulation in non-alcoholic fatty liver disease. *J Gastroenterol* **48**:434–441.

Krishnan S, Ding Y, Saedi N, Choi M, Sridharan GV, Sherr DH, Yarmush ML, Alaniz RC, Jayaraman A, and Lee K (2018) Gut microbiota-derived tryptophan metabolites modulate inflammatory response in hepatocytes and macrophages. *Cell Rep* **23**:1099–1111.

Larigot L, Juricek L, Dairou J, and Coumoul X (2018) AhR signaling pathways and regulatory functions. *Biochim Open* **7**:1–9.

Le MH, Yeo YH, Li X, Li J, Zou B, Wu Y, Ye Q, Huang DQ, Zhao C, Zhang J et al. (2021) 2019 global NAFLD prevalence: A systematic review and meta-analysis. *Clin Gastroenterol Hepatol* S1542-3565(21)01280-5.

Lee JH, Wada T, Febbraio M, He J, Matsubara T, Lee MJ, Gonzalez FJ, and Xie W (2010) A novel role for the dioxin receptor in fatty acid metabolism and hepatic steatosis. *Gastroenterology* **139**:653–663.

Liu Y, She W, Wang F, Li J, Wang J, and Jiang W (2014) 3, 3′-Diindolylmethane alleviates steatosis and the progression of NASH partly through shifting the imbalance of Treg/Th17 cells to Treg dominance. *Int Immunopharmacol* **23**:489–498.

Lowe MM, Mold JE, Kanwar B, Huang Y, Louie A, Pollastri MP, Wang C, Patel G, Franks DG, Schlezinger J et al. (2014) Identification of cinnabarinic acid as a novel endogenous aryl hydrocarbon receptor ligand that drives IL-22 production. *PLoS One* **9**:e87877.

Ma C, Marlowe JL, Puga A. (2009) The aryl hydrocarbon receptor at the crossroads of multiple signaling pathways. *EXS* **99**:231–257.

Ma Q (2001) Induction of CYP1A1. The AhR/DRE paradigm: transcription, receptor regulation, and expanding biological roles. *Curr Drug Metab* **2**:149–164.
Michel MC, Murphy TJ, and Motulsky HJ (2020) New author guidelines for displaying data and reporting data analysis and statistical methods in experimental biology. *J Pharmacol Exp Ther* **372**:136–147.
Mimura J and Fujii-Kuriyama Y (2003) Functional role of AhR in the expression of toxic effects by TCDD. Biochimica Et Biophysica Acta (BBA)-. *General Subjects* **1619**:263–268.
Mitchell KA, Lockhart CA, Huang G, and Elferink CJ (2006) Sustained aryl hydrocarbon receptor activity attenuates liver regeneration. *Mol Pharmacol* **70**:163–170.
Muku GE, Blazanin N, Dong F, Smith PB, Thiboutot D, Gowda K, Amin S, Murray IA, and Perdew GH (2019) Selective Ah receptor ligands mediate enhanced SREBP1 proteolysis to restrict lipogenesis in sebocytes. *Toxicol Sci* **171**:146–158.
Murray IA and Perdew GH (2020) How ah receptor ligand specificity became important in understanding its physiological function. *Int J Mol Sci* **21**:9614.
Nault R, Fader KA, Ammendolia DA, Dornbos P, Potter D, Sharratt B, Kumagai K, Harkema JR, Lunt SY, Matthews J et al. (2016) Dose-dependent metabolic reprogramming and differential gene expression in TCDD-elicited hepatic fibrosis. *Toxicol Sci* **154**:253–266.
Nebert DW, Puga A, and Vasiliou V (1993) Role of the Ah receptor and the dioxin-inducible [Ah] gene battery in toxicity, cancer, and signal transduction. *Ann N Y Acad Sci* **685**:624–640.
Ochi T, Kawaguchi T, Nakahara T, Ono M, Noguchi S, Koshiyama Y, Munekage K, Murakami E, Hiramatsu A, Ogasawara M et al. (2017) Differences in characteristics of glucose intolerance between patients with NAFLD and chronic hepatitis C as determined by CGMS. *Sci Rep* **7**:10146.
Park KT, Mitchell KA, Huang G, and Elferink CJ (2005) The aryl hydrocarbon receptor predisposes hepatocytes to Fas-mediated apoptosis. *Mol Pharmacol* **67**:612–622.
Patil NY, Tang H, Rus I, Zhang K, and Joshi AD (2022) Decoding cinnabarinic Acid–Specific stanniocalcin 2 induction by aryl hydrocarbon receptor. *Mol Pharmacol* **101**:45–55.
Pierre S, Chevallier A, Teixeira-Clerc F, Ambolet-Camoit A, Bui LC, Bats AS, Fournet JC, Fernandez-Salguero P, Aggerbeck M, Lotersztajn S et al. (2014) Aryl hydrocarbon receptor-dependent induction of liver fibrosis by dioxin. *Toxicol Sci* **137**:114–124.
Postic C and Girard J (2008) The role of the lipogenic pathway in the development of hepatic steatosis. *Diabetes Metab* **34**:643–648.
Probst MR, Reisz-Porszasz S, Agbunag RV, Ong MS, and Hankinson O (1993) Role of the aryl hydrocarbon receptor nuclear translocator protein in aryl hydrocarbon (dioxin) receptor action. *Mol Pharmacol* **44**:511–518.
Rada P, González-Rodríguez Á, García-Monzón C, and Valverde ÁM (2020) Understanding lipotoxicity in NAFLD pathogenesis: is CD36 a key driver? *Cell Death Dis* **11**:802.
Reyes H, Reisz-Porszasz S, and Hankinson O (1992) Identification of the Ah receptor nuclear translocator protein (Arnt) as a component of the DNA binding form of the Ah receptor. *Science* **256**:1193–1195.
Safe S, Han H, Goldsby J, Mohankumar K, and Chapkin RS (2018) Aryl hydrocarbon receptor (AhR) ligands as selective AhR modulators: Genomic studies. *Curr Opin Toxicol* **11-12**:10–20.
Savouret JF, Berdeaux A, and Casper RF (2003) The aryl hydrocarbon receptor and its xenobiotic ligands: a fundamental trigger for cardiovascular diseases. *Nutr Metab Cardiovasc Dis* **13**:104–113.
Shetty A and Syn WK (2019) Health and economic burden of nonalcoholic fatty liver disease in the united states and its impact on veterans. *Fed Pract* **36**:14–19.
Tilg H and Moschen AR (2010) Evolution of inflammation in nonalcoholic fatty liver disease: the multiple parallel hits hypothesis. *Hepatology* **52**:1836–1846.
Wada T, Sunaga H, Miyata K, Shirasaki H, Uchiyama Y, and Shimba S (2016) Aryl hydrocarbon receptor plays protective roles against high fat diet (HFD)-induced hepatic steatosis and the subsequent lipotoxicity via direct transcriptional regulation of Socs3 gene expression. *J Biol Chem* **291**:7004–7016.
Walisser JA, Glover E, Pande K, Liss AL, and Bradfield CA (2005) Aryl hydrocarbon receptor-dependent liver development and hepatotoxicity are mediated by different cell types. *Proc Natl Acad Sci USA* **102**:17858–17863.
White DL, Kanwal F, El–Serag HB. (2012) Association between nonalcoholic fatty liver disease and risk for hepatocellular cancer, based on systematic review. *Clin Gastroenterol Hepatol* **10**:1342–1359.
Wilson CG, Tran JL, Erion DM, Vera NB, Febbraio M, and Weiss EJ (2016) Hepatocyte-specific disruption of CD36 attenuates fatty liver and improves insulin sensitivity in HFD-fed mice. *Endocrinology* **157**:570–585.
Wójcik-Cichy K, Koślińska-Berkan E, and Piekarska A (2018) The influence of NAFLD on the risk of atherosclerosis and cardiovascular diseases. *Clin Exp Hepatol* **4**:1–6.
Wright EJ, De Castro KP, Joshi AD, and Elferink CJ (2017) Canonical and non-canonical aryl hydrocarbon receptor signaling pathways. *Curr Opin Toxicol* **2**:87–92.
Wu R, Zhang L, Hoagland MS, and Swanson HI (2007) Lack of the aryl hydrocarbon receptor leads to impaired activation of AKT/protein kinase B and enhanced sensitivity to apoptosis induced via the intrinsic pathway. *J Pharmacol Exp Ther* **320**:448–457.
Xia H, Zhu X, Zhang X, Jiang H, Li B, Wang Z, Li D, and Jin Y (2019) Alpha-naphthoflavone attenuates non-alcoholic fatty liver disease in oleic acid-treated HepG2 hepatocytes and in high fat diet-fed mice. *Biomed Pharmacother* **118**:109287.
Xu N, Luo H, Li M, Wu J, Wu X, Chen L, Gan Y, Guan F, Li M, Su Z et al. (2021) β-patchoulene improves lipid metabolism to alleviate non-alcoholic fatty liver disease via activating AMPK signaling pathway. *Biomed Pharmacother* **134**:111104.
Zeng L, Tang WJ, Yin JJ, and Zhou BJ (2014) Signal transductions and nonalcoholic fatty liver: a mini-review. *Int J Clin Exp Med* **7**:1624–1631.
Zhang C and Yang M (2021) Current options and future directions for NAFLD and NASH treatment. *Int J Mol Sci* **22**:7571.
Zhao J, Jiao Y, Song Y, Liu J, Li X, Zhang H, Yang J, and Lu Y (2018) Stanniocalcin 2 ameliorates hepatosteatosis through activation of STAT3 signaling. *Front Physiol* **9**:873.
Zhou H, Wu H, Liao C, Diao X, Zhen J, Chen L, and Xue Q (2010) Toxicology mechanism of the persistent organic pollutants (POPs) in fish through AhR pathway. *Toxicol Mech Methods* **20**:279–286.
Zhu XY, Xia HG, Wang ZH, Li B, Jiang HY, Li DL, Jin R, and Jin Y (2020) In vitro and in vivo approaches for identifying the role of aryl hydrocarbon receptor in the development of nonalcoholic fatty liver disease. *Toxicol Lett* **319**:85–94.

Address correspondence to: Dr. Aditya D. Joshi, Department of Pharmaceutical Sciences, University of Oklahoma Health Sciences Center, Oklahoma City, OK 73117. E-mail: Aditya-joshi@ouhsc

SUPPLEMENTAL DATA

Article Title: Cinnabarinic acid provides hepatoprotection against non-alcoholic fatty liver disease

Authors' Names: Nikhil Y. Patil, Iulia Rus, Emma Downing, Ashok Mandala, Jacob E. Friedman, Aditya D. Joshi

Journal Name: Journal of Pharmacology and Experimental Toxicology

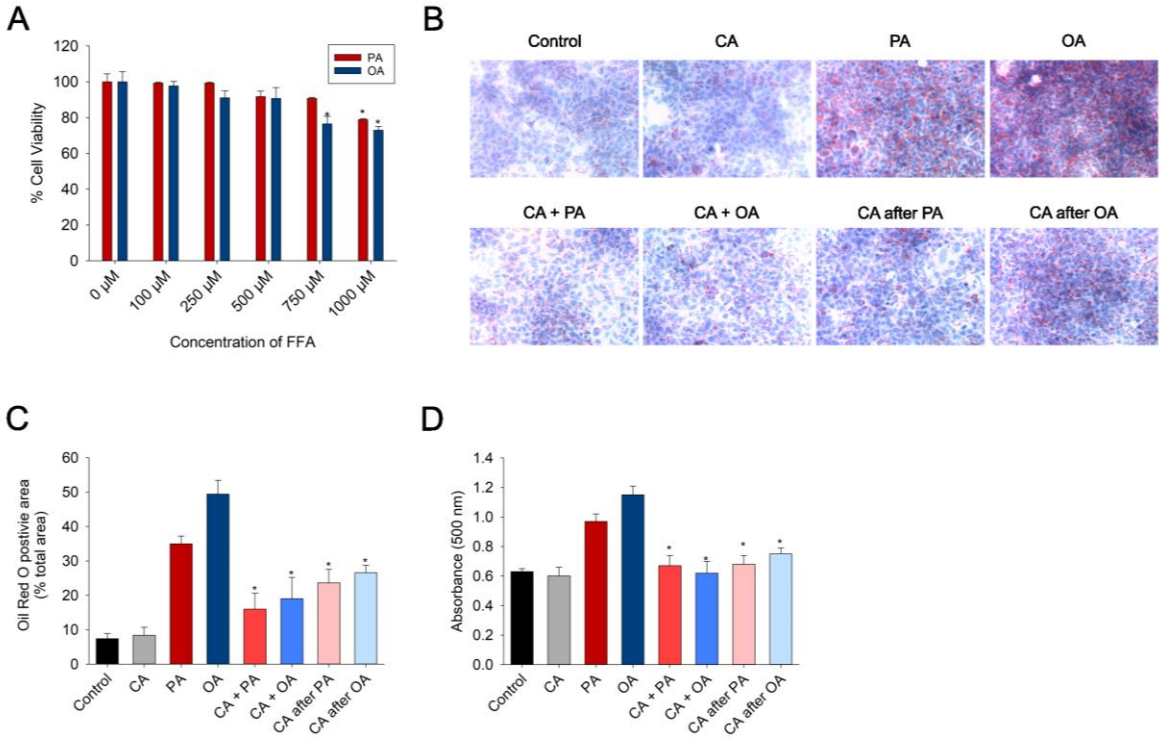

Supplemental Figure 1. Determination of (A) cell viability of AML12 cells treated with different concentrations of palmitic acid (PA) and oleic acid (OA) for 24 hrs. Cell viability was measured by a luminescent assay and expressed relative to BSA-treated control. Data are represented as mean ± SD (n=3). *p<0.05 compared to control group. (B) CA protects against palmitic acid (PA)/oleic acid (OA)-induced steatosis. Representative images of oil red O stained AML12 cells treated with 500µM BSA + DMSO (control), 30µM CA, 500µM PA, 500µM OA, 30µM CA+ 500µM PA/OA, 30µM CA after 500µM PA/OA. (C) Quantification of oil red O-stained images; area of stained lipid droplets was determined using ImageJ and normalized to the total area (3 images per treatment) (D) quantification of accumulated oil red O by colorimetry; absorbance measured at 500 nm. Data are represented as mean ± SD (n=3). *p<0.05 compared to PA/OA-only treatment group.

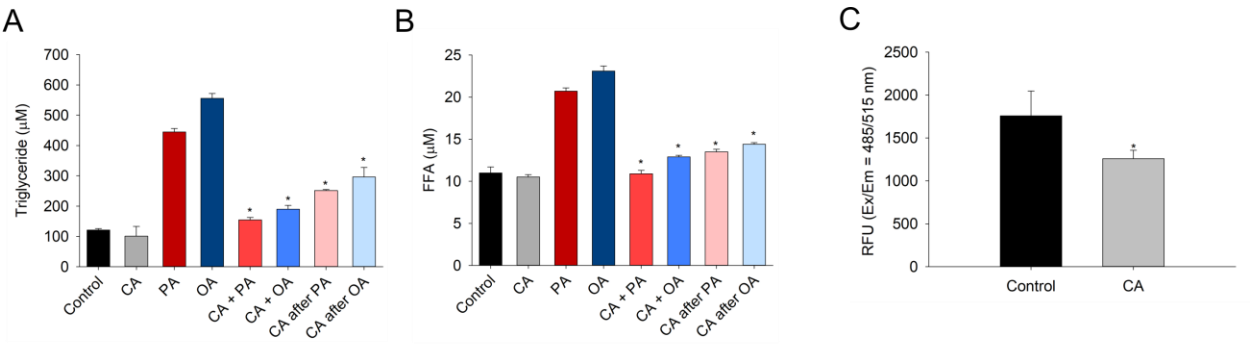

Supplemental Figure 2. Quantification of (A) triglyceride, (B) free fatty acid and (C) free fatty acid uptake in AML12 cells treated with 500μM BSA + DMSO (control), 30μM CA, 500μM PA, 500μM OA, 30μM CA+ 500μM PA/OA, 30μM CA after 500μM PA/OA. Triglyceride content was measured using luminescence assay, whereas free fatty acid content and free fatty acid uptake was determined fluorometrically. Data are represented as mean + SD (n=3). *$p<0.05$ compared to PA/OA-only treatment group.

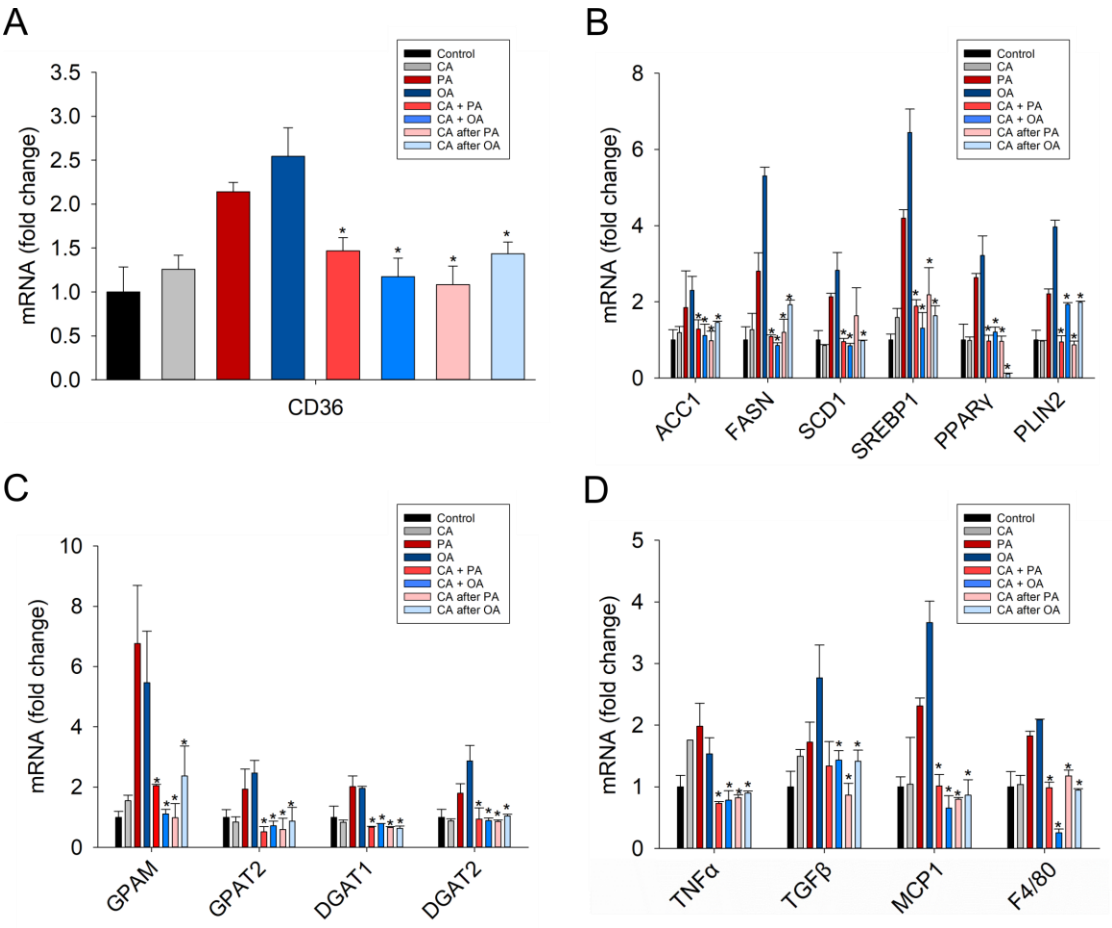

Supplemental Figure 3. Expression of mRNAs encoding genes involved in (A) free fatty acid transport, (B) fatty acid synthesis, (C) triglyceride synthesis, and (D) inflammation. AML12 cells were treated with 500μM BSA+ DMSO (control), 30μM CA, 500μM PA, 500μM OA, 30μM CA+ 500μM PA/OA , 30μM CA after 500μM PA/OA. mRNA message was analyzed by qRT-PCR and normalized to 18S rRNA. Results are expressed as fold of the value found in control treatment arbitrarily set at 1. For statistical analysis, a mixed-effects multivariate ANOVA (MANOVA) model was used. After an overall significant F test from MANOVA model, the post hoc multiple-comparison tests were performed for the pre-specified comparisons adjusted by Tukey procedure. Data are represented as mean ± SD (n=3). *p<0.05 compared to PA/OA-only treatment group.

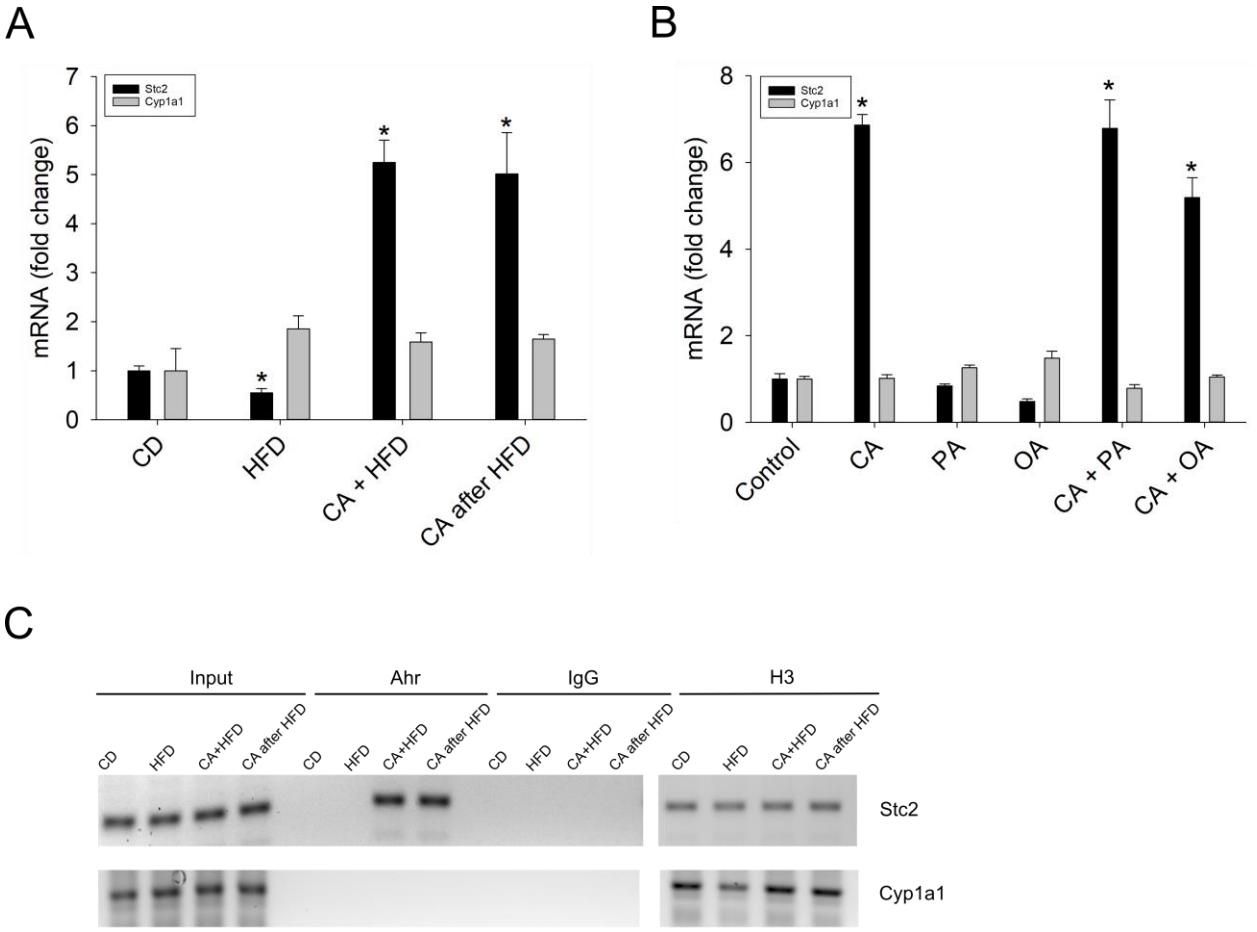

Supplemental Figure 4. CA treatment activates AhR signaling by upregulating Stc2 expression. mRNA expression of Stc2 and Cyp1a1 measured by qRT-PCR in (A) *in vivo* and (B) *in vitro* models of NAFLD, normalized to 18S rRNA. Data are represented as mean ± SD. *p<0.05 compared to control diet(CD)/control group. (B) ChIP analysis of AhR binding to Stc2 and Cyp1a1 promoters in mice liver tissue. IgG and histone H3 antibodies were used as negative and positive controls respectively. The XRE clusters in the Stc2 and Cyp1a1 promoters (Patil et al., 2022) were PCR-amplified and PCR products separated and visualized on 5% polyacrylamide gels.

Supplemental Table 1. Primer sequences for quantitative RT-PCR

Species	Gene	Forward Primer	Reverse primer
Human	ACAA1	GCGGTTCTCAAGGACGTGAAT	GTCTCCGGGATGTCACTCAGA
Mouse	ACAA1	CCAACATTGCTGGTGGCATC	CCCATCCCAGACAGGGACAT
Human	ACADL	TGCAATAGCAATGACAGAGCC	CGCAACTACAATCACAACATCAC
Mouse	ACADL	TGCACACATACAGACGGTGC	CATGGAAGCAGAACCGGAGT
Human	ACC1	GCAGGTCACACGTCTCTTTAT	CCAGCCTGTCATCCTCAATATC
Mouse	ACC1	TAACAGAATCGACACTGGCTGGCT	ATGCTGTTCCTCAGGCTCACATCT
Human	ACOX1	TGCTGATGAAGTATGCCCAGGTGA	TCCCACAAGGAAGGACCTGACAAA
Mouse	ACOX1	TCATGTGGTTTAAAAACTCTGTGC	GCAGGAACATGCCCAAGTGA
Human	CD36	AAACGGCTGCAGGTCAACCTATTG	TCATCACCAATGGTCCCAGTCTCA
Mouse	CD36	TCATGCCAGTCGGAGACATGCTTA	AACTGTCTGTACACAGTGGTGCCT
Human	CPT1A	GCAAAGGCGACATCAATCCGAACA	ACCAAAGGCTACGAATGGGAAGGA
Mouse	CPT1A	GTCCCTCCAGCTGGCTTATC	CATGCGGCCAGTGGTGTCTA
Human	CPT2	GCTGCCTATTCCCAAACTTG	CATGCAGTTCTTTTCCAATCCC
Mouse	CPT2	TCGTACCCACCATGCACTAC	CTTCTGTCTTCCTGAACTGGCT
Human	DGAT1	CCTACCGCGATCTCTACTACTT	GGGTGAAGAACAGCATCTCAA
Mouse	DGAT1	AACCTGGCCACAATCATCTGCTTC	ATGATGCCAGAGCAAACACGGAAC
Human	DGAT2	ATTGCTGGCTCATCGCTGT	GGGAAAGTAGTCTCGAAAGTAGC
Mouse	DGAT2	TTCTGCACAGACTGCTGGCTGATA	TCACCAGCTGGATGGGAAAGTAGT
Human	F4/80	CAGACCAAGGAGTGGAATGTAG	GCCTTCTGGATTGGGATGAA
Mouse	F4/80	TCAAATGGATCCAGAAGGCTCCCA	TGCACTGCTTGGCATTGCTGTATC
Human	FASN	TACGACTACGGCCCTCATTT	CCATGAAGCTCACCCAGTTATC
Mouse	FASN	GGTGTGGTGGGTTTGGTGAATTGT	TTGCTGAGGTTGGACAGCAGGATA
Human	GPAM	CTAGCAAGTCCTGTGCCATTA	CGACCAATGTGGAGAGATCAA
Mouse	GPAM	ATGAAACGCACACAAGGCAC	CCCTTATGGACGTCTCGCTC
Human	GPAT2	TGTGGTCGTCAGGCTTTGG	GGTCCGTTATGCTTCTGTGGA
Mouse	GPAT2	GCACATACCCACCAGTTTTGA	AGGATACGCTGTACCTCTTTCT
Human	MCP1	TCGCTCAGCCAGATGCAATCAATG	CACAGCTTCTTTGGGACACTTGCT
Mouse	MCP1	TCACCTGCTGCTACTCATTCACCA	AGCACAGACCTCTCTCTTGAGCTT
Human	MOGAT1	AGGCCATGAAGGTAGAGTTTG	CCCGAGCAGCAGGTATTT
Human	PLIN2	TTGCAGTTGCCAATACCTATGC	CCAGTCACAGTAGTCGTCACA
Mouse	PLIN2	CAGCTCTCCTGTTAGGCGT	CGGAGGACACAAGGTCGTAG
Human	PPARγ	TACTGTCGGTTTCAGAAATGCC	GTCAGCGGACTCTGGATTCAG
Mouse	PPARγ	AGGGCGATCTTGACAGGAAAGACA	AAATTCGGATGGCCACCTCTTTGC
Human	RNA18S	GGACAGGATTGACAGATTGAT	AGTCTCGTTCGTTATCGGAAT
Mouse	RNA18S	CTCAACACGGGAAACCTCAC	CGCTCCACCAACTAAGAACG
Human	SCD1	AACTGGTGATGTTCCAGAGGAGGT	CGCAAGAAAGTGGCAACGAACACA
Mouse	SCD1	CAGGTTTCCAAGCGCAGTTC	ACTGGAGATCTCTTGGAGCA
Human	SREBP1C	GGAGCCATGGATTGCACTTT	TCCCAGCATAGGGTGGGTCAAATA

Mouse	SREBP1C	GGAGCCATGGATTGCACATT	GGCCCGGGAAGTCACTGT
Human	TGFβ	GGAAATTGAGGGCTTTCGCC	CCGGTAGTGAACCCGTTGAT
Mouse	TGFβ	TAAAGAGGTCACCCGCGTGCTAAT	ACTGCTTCCCGAATGTCTGACGTA
Human	TNFα	GCCCATGTTGTAGCAAACCCTCAA	GTTATCTCTCAGCTCCACGCCATT
Mouse	TNFα	TAGCCCACGTCGTAGCAAAC	ACAAGGTACAACCCATCGGC

Supplemental Table 2. Primer sequences for ChIP

Species	**Gene**	**Forward Primer**	**Reverse primer**
Mouse	CYP1A1	CTATCTCTTAAACCCCACCCCAA	CTAAGTATGGTGGAGGAAAGGGTG
Mouse	STC2	CTCAGTCCATTCGGCCATTGCCC	AGGAAGCGGAGCGCCTCCGC